4 RESULTS

4.1 Yeast two- hybrid screens with DAF-12 bait plasmids

In order to define DAF-12 transcriptional complexes, we searched for DAF-12 interacting proteins by the yeast two-hybrid method. We screened three DAF-12 bait constructs against two different random- and oligo dT primed *C. elegans* mixed stage cDNA libraries, one provided by R. Barstead and another commercially available from GIBCO. The DAF-12 bait constructs encoded a truncated version of DAF-12, comprising ligand binding domain and hinge region (DAF-12HL), DAF-12 isoform A1 and DAF-12 isoform A3 (Figure 7).

In total, we found 22 interactors (Tables 5-8) seven of which were selected for further study (highlighted in the Tables 5-8, Figure 9). We selected those clones where protein BLAST alignments revealed homologies with proteins acting in nuclear complexes. We also evaluated candidates using protein analysis programs like Pfam and Psort to search for functional domains typical of transcriptional complexes such as zinc fingers and nuclear localisation sites.

First, we screened DAF-12HL against an oligo-dT primed mixed stage cDNA library, provided by R. Barstead (Figure 8, Screen I). In total, we obtained 102 His^+, Ura^+ clones.

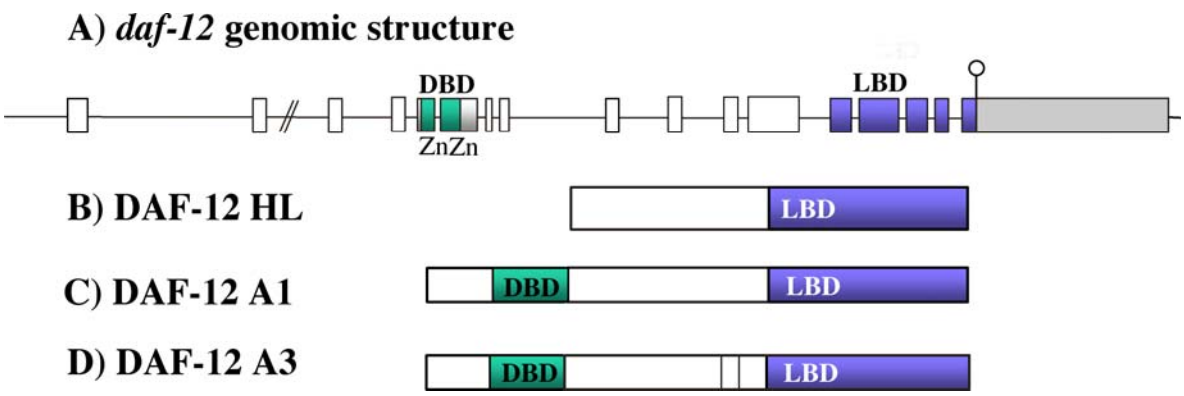

Figure 7) *daf-12* genomic structure and *daf-12* cDNA used for the Yeast Two-Hybrid Screens. A) *daf-12* genomic structure. DBD with zinc fingers drawn in green, LBD in blue, 3' UTR in gray, stop codon. dash andcircle. **B)** DAF-12HL containing hinge and LBD **C)** DAF-12 isoform A1 **D)** DAF-12 isoform A3. Isoforms A1 and A3 differ by 16 aa due to alternate splicing within the exon 12. *daf-12* cDNAs were cloned into the shuttle vector pBTM117c encoding a lexA fusion protein under the control of the yeast ADH-1 promotor.

ß-galactosidase tests for expression of the lacZ reporter gene reduced the number of candidate clones to 35. 16 of these were transformed into *E. coli* and analysed by sequencing, revealing five different genes. We found four independent clones of the gene F07A11.6 (Table 5, Figure 11), a putative transcriptional corepressor showing regions homologous to mammalian and *Drosophila* proteins, which we analyzed below in more detail (see parts 2-7 of this chapter).

Screens with the same bait against a random primed cDNA library from GIBCO (Figure 8, Screen II) revealed 237 clones. 112 clones were analyzed by restriction digestion, eleven of those have been sequenced and two of them passed our evaluation criteria (Table 6). These clones, F4611.2 and M03F4.7, were isolated only once. F4611.2 encodes a homolog of a human cold shock domain protein. Cold shock domain proteins contain specific DNA binding regions (Doninger et al., 1992) and are regarded as transcriptional regulators (Obokata, 1991). The DAF-12– F4611.2 interaction domain spans much of the predicted cold shock domain (Figure 9A). M03F4.7 encodes a calumenin-like calcium binding protein showing high homology to CBP50 protein, a *Drosophila* DNA supercoiling factor, and to a mammalian vitamin D receptor-associated factor. M03F4.7 contains several EF hand motifs (PF00036), which are calcium-binding motifs found in calcium signaling or buffering transport proteins. The DAF-12-M03F4.5 interaction domain includes all 5 predicted EF hand domains (Figure 9B).

To obtain a broader spectrum of putative DAF-12 interacting proteins, we performed yeast-two hybrid screens using bait constructs encodin g DAF-12 isoforms A1 and A3 (Figure 7C, D). Both were tested negative for autoactivation. A screen with DAF-12A1 as bait against an oligo-dT primed cDNA library from R. Barstead (Figure 8, Screen III) revealed only eight independent clones. Two of them encoded T05C1.6, which contains weak homology to suppressor protein SPT23 from *Neurospora crassa*. Previous RNAi studies with T05C1.6 revealed an embryonic lethality of 11% (Maeda et al., 2001). T05C1.6 contains a conserved IPT/TIG domain (PF01833), a motif found in intracellular transcription factors involved in DNA binding (Collesi et al., 1996). Another predicted PFAM domain in T05C1.6 is the ankyrin repeat (PF00023), which is present in a large number of functionally diverse eukaryotic proteins (Batchelor et al., 1998; Gorina, 1996). However, neither the ankyrin domain nor the IPT/TIG domain are contained within the interacting region (Figure 9C).

Another three clones encoded M04B2.1, a homolog to a human C2H2 type zinc finger protein (Table 7, Figure 9D) (Evans and Hollenberg, 1988). The region of interaction

Screen I	**Screen II**
Yeast strain L40ccu/pBTM117c- DAF-12HL transformed with 100 µg *C. elegans* cDNA (Barstead) Transformation efficiency: $9.3x10^6$ / µg DNA ↓ 102 tranformants grown on SD medium -Leu-Trp-His-Ura ↓ 35 positives in ß-galactosidase tests Yeast DNA preps, transformation into E.coli ↓ 16 transformants sequence analyses ↓ 5 genes, e.g. ***din-1***	Yeast strain L40ccu/pBTM117c-DAF-12HL transformed with 100 µg *C. elegans* cDNA (GIBCO) Transformation efficiency: $8.2x10^6$ / µg DNA ↓ 237 tranformants grown on SD medium -Leu-Trp-His-Ura ↓ Yeast DNA preps, 112 transformants in *E.coli* analyzed by HindIII digestion 11 clones with different restriction patterns ↓ sequence analyses ↓ 11 genes, e.g. **F46F11.2; M03F4.7**
Screen III	**Screen IV**
Yeast strain L40ccu/pBTM117c-DAF-12A1 transformed with 100 µg *C. elegans* cDNA (Barstead) Transformation efficiency: $3.4x10^7$/ µg DNA ↓ 8 tranformants grown on SD medium -Leu-Trp-His-Ura ↓ sequence analyses ↓ 2 genes, **T05C1.6 and M04B2.1**	Yeast strain L40ccu/pBTM117c-DAF-12A3 transformed with 100 µg *C. elegans* cDNA (Barstead) Transformation efficiency: $9.1x10^6$ / µg DNA ↓ 550 tranformants grown on SD medium -Leu -Trp-His-Ura ↓ Yeast DNA preps, transformation into E.coli 48 clones, restriction and sequence analyses ↓ 5 genes, e.g. ***ptr-23*, R144.7**

Figure 8) Schematic outline of the four yeast two-hybrid screens with DAF-12 bait constructs screened against *C. elegans* mixed stage cDNA libraries.

between DAF-12 and M04B2.1 comprises the three N-terminal C2H2 zinc finger motifs out of six within the predicted protein. M04B2.1 corresponds to an identified *C. elegans* mutant locus *mep-1* (MOG interacting and Ectopic P-granules) that binds MOG DEAH box proteins (Graham and Kimble, 1993). Previous RNAi studies revealed an early larval arrest (Belfiore et al., 2002).

When we used the DAF-12 isoform A3 as bait to screen the same library (Figure 8, Screen IV), we obtained approximately 550 positives, 48 of them were examined further by restriction analysis. We found three clones encoding ZK270.1= *ptr-23,* which shows embryonic lethal phenotype (Gonczy et al., 2000). The DIN-1 R144.7 interaction domain similarity to the human Niemann-Pick C disease protein and to numerous patched-related

Table 5) Results of the yeast-two hybrid screen I with a bait construct encoding DAF-12HL against a random primed cDNA library (R. Barstead).

Gene Map position	Number of clones, Position in cosmid	BLAST with entire proteins	E-value	Comments
F07A11.6 ***din-1*** **II, 4.93**	**4 clones** **29025-32118** **32398-33144** **32503-33139** **32415-33144**	**a) SMRT/ HDAC1 Associated Repressor protein *(Homo sapiens)*** **b) Msx 2 interacting nuclear target protein MINT (*Mus musculus)*** **c) Split ends protein SPEN *(Drosophila melanogaster)***	**5e-09** **4e-10** **3e-06**	RNAi suppresses *daf-2, daf-7, daf-11* Daf-c and *daf-9, daf-12* Daf-c and Mig phenotypes
T09E8.2 *him-17* V, -4.92	2 clones 9873-10384 9818-10345	a) Myosin heavy chain, gizzard smooth muscle *(Gallus gallus)* b) Moe gene product (*alt-1*) *(Drosophila melanogaster)*	4e-04 0.039	RNAi: - Psort: 39.1% nuclear 21.7% membrane
B0228.4 II, 0.51	3 clones 3782-4373; 3780-4557 3873-4444	Transcription termination factor RHO *(Brucella melitensis)*	0.32	RNAi: - Psort: 65.2 % nuclear
T13B5.1 *snf-3* II, 13.39	3clones, 679-2090	a) Solute carrier family 6 / neurotransmitter *(Homo sapiens)* b) Na^+ / Cl^- betaine / GABA-transporter (rat/mouse / h. s.)	e-116 e-116	RNAi: -
ZC8.4 X, -6.34	1 clone 12441-13781	a) Strong similarity to *Onchocerca volvulus* major antigen OVT-1 b) Myosin-like protein PUMA1 *(Parascaris univalens)* c) rho/rac-interacting citron kinase *(Mus musculus)* d) Intracellular protein transport protein USO1 *(Saccharomyces cerevisiae)*	e-102 5e-90 3e-08 4e-08	RNAi: -

proteins from different species. The region of interaction with DAF-12 spans the transmembrane domains within ZK270.1 (Figure 9E), which are supposed to play key roles in different aspects of cholesterol homeostasis or cholesterol-linked signaling (Loftus, 1997). We also detected one clone encoding R144.7, which is highly homologous to an RNA-binding Lupus La protein from *Drosophila*. Previous studies with RNAi revealed anincludes a conserved tandem motif of unknown function (Figure 9F).

In summary, in the four screens for DAF-12 interacting factors we identified putative repressor protein F07A11.6 and T05C1.6, transcriptional regulators F46F11.2 and M04B2.1, an EF hand containing protein M03F4.7, ZK270.1, a transmembrane protein possibly involved in cholesterol trafficking and R144.7, an RNA binding factor that might be involved in RNA metabolism.

Table 6) Results of the yeast-two hybrid screen II with a bait construct encoding DAF-12HL LBD against a random primed cDNA library (GIBCO).

Gene **Map position**	**Number of clones,** **Position in cosmid**	**BLAST with entire proteins**	**E-value**	**Comments**
F46F11.2 I, 5.61	**1 clone** **19228-18410**	**Cold-shock DNA binding domain containing protein *(Homo sapiens)***	**1e-19**	**RNAi: n.d.**
M03F4.7 **X, -6.42**	**1 clone** **22760-22179**	**a) Calumenin *(Homo sapiens)*** **b) CBP-50 protein *(Rattus norvegicus)*** **c) Supercoiling factor(*Drosophila melanogaster)*** **d) Vitamin D receptor associated factor1 *(Mus musculus)***	**8e-81** **9e-80** **1e-76** **1e-46**	**RNAi: -**
F31E3.5 *eft-3* II, -0.83	1 clone 7895-7566	elongation factor 1 alpha-2 *(Homo sapiens)*	0.0	RNAi: -
B0511.5 I, 10.6	1 clone 3431-5032	a) Cuticulin-1 precursor (*C. elegans*) b) SP71 gene product *(Drosophila melanogaster)*	9e-30 3e-09	RNAI: -
C44C10.1 X, 11.71	1 clone 28649-29375	cuticular collagen *(Ostertagia circumcincta)*	3e-26	RNAi: -
F09G2.2 V, 7.199	1 clone 30856-31645	a) CGI-57 protein *(Homo sapiens)* b) Regulatory protein-like *(Arabidopsis thaliana)* c) Putative PREG1-like negative regulator *(Arabidopsis thaliana)*	4e-14 0.005 0.001	RNAi: -
C53B4.4 IV, 3.96	1 clone 12973-13841	a) CG10362 gene product *(Drosophila melanogaster)* c) Hypothetical protein DKFZ p434B0328.1 *(Homo sapiens)*	2e-40 7e-17	RNAi: n.d.
T07C4.1 III, 10.35	102 clones 33477-32766	a) Uridine monophosphate synthetase	5e-86	RNAi: n.d.
C14A4.3 II, 10.58	1 clone 4482-4546	CG11851 gene product *(Drosophila melanogaster)*	1e-88	RNAi: n.d.
K10B3.8 *gpd-2* X, 3.12	1 clone 9320-11292	Glyceralaldehyde-3-phosphate dehydrogenase	1e-160	RNAi: - embryonic lethal (22%)(Maeda et al., 2001)
Y6D1A.1 II, 11.82	1 clone 6476-6096	a) T27D12.4.p *(C. elegans)* b) *mrp-14*, *(C. elegans)*	1e-14 7e-04	RNAi: -

Table 7) Results of the yeast-two hybrid screens III with a bait constructencoding DAF-12 isoform A1 against a random primed cDNA library (R. Barstead).

Gene Map position	Number of clones, Position in cosmid	BLAST with entire proteins	E-value	Comments
T05C1.6 **II, 4.499**	**2 clones** **32712-32685** **32216-32725,**	**a) (AL833974) hypothetical protein (*Homo sapiens*)** **b) Related to suppressor protein SPT23 (*Neurospora crassa)*** **c) Transcription factor-like protein (*Arabidopsis thaliana)***	**2e-18** **7e-04** **0.003**	**RNAi: -** **11% embryonic lethal (A et al., 2001)** **Psort:** **52.2% nuclear** **17%mitochondrial**
M04B2.1 ***mep-1*** **IV, 5.01**	**4 clones** **21275-21518** **22836-22574** **21230-21516** **21275-21514**	**KIAA0478 (C2H2 type zinc finger protein (isoform 1) *(Homo sapiens)***	**6e-04**	**RNAi: -** **early larval arrest(Belfiore et al., 2002)**

Table 8) Results of the yeast-two hybrid screen IV with a bait construct encoding DAF-12 isoform A3 against a random primed cDNA library (R. Barstead)

Gene Map position	Number of clones, Position in cosmid	BLAST with entire proteins	E-value	comments
ZK270.1 ***ptr-23*** **I, 14.92**	**3 clones** **30177-30447** **28751-28982** **130166-30437**	**a) F44F4.4 - Caenorhabditis elegans Similar to transmembranous domains within HMG-CoA reductase and the *Drosophila* patched protein** **b) R09H10.4 similarity to human Niemann-Pick C disease protein and numerous patched-relatedproteins *(C. elegans)***	**e-155** **e-148**	**RNAi: -**
R144.7 **III, 5.00**	**1 clone,** **14694-14967**	**La related protein *(Drosophila melanogaster)***	**5e-52**	**RNAi: n.d.** **embryonic lethal (Gonczy et al., 2001)**
D2085.5 II, 8.67	3 clones 29066-29355 29066-29356 29127-29369	KIAA1219 *(Homo sapiens)*	1e-34	RNAi: n.d. 65,2 % nuclear 17,4 %cyto-plasmic
C36B1.1 *cle-1* I, 8.71	2 clones F39H11 10039-9764	Collagen, type XV, alpha 1; Collagen XV, alpha-1 polypeptide (*H. sapiens)*	6e-36	RNAi: n.d. Psort: 47.8% nuclear 17% mitochondrial

A) F46F11.2 (268 aa)

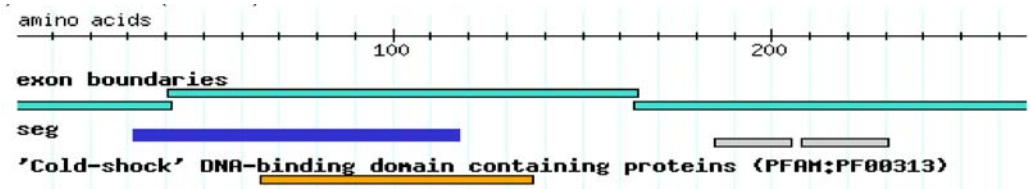

Protein BLAST with F46F11.2 - DAF-12 interaction region; aa 30-118

Top scores:	**E-value**
DNA-binding protein A *(Homo sapiens)*	4e-10
'Cold-shock' DNA-binding domain *(Caenorhabditis elegans)*	3e-10
RNA binding protein MSY4 *(Mus musculus)*	6e-10
mRNA-binding protein p54 *(Xenopus laevis)*	6e-10
Germ cell specific Y-box binding protein *(Homo sapiens)*	7e-09

B) M03F4.7 (314 aa)

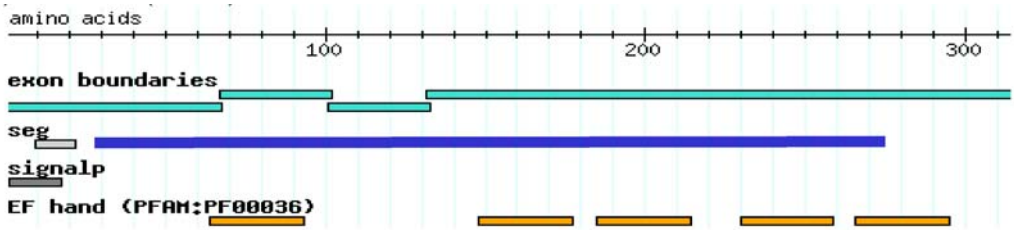

Protein BLAST with M03F4.7 - DAF-12 interaction region; aa 30-278

Top scores:	**E-value**
Calcium binding protein *(Caenorhabditis elegans)*	2e-108
Calumenin *(Homo sapiens)*	9e-46
CBP-50 protein *(Rattus norvegicus)*	3e-43
DNA supercoiling factor *(Bombyx mori)*	2e-43

C) T05C1.6 (950 aa)

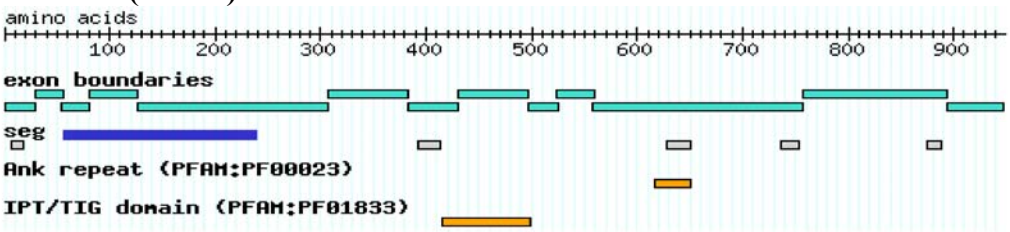

Protein BLAST with T05C1.6 - DAF-12 interaction region; aa 72-251

Top scores:	**E-value**
hypothetical protein *(Homo sapiens)*	7e-20
calmodulin-binding transcription activator *(Brassica napus)*	2e-07
transcription factor-like protein *(Arabidopsis thaliana)*	5e-04

D) M04B2.1 (854 aa)

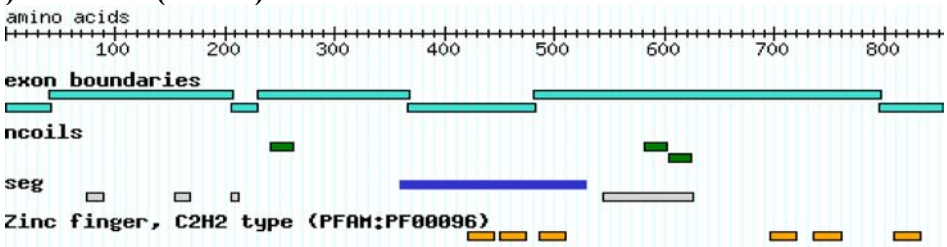

Protein BLAST with MO4B2.1 - DAF-12 interaction region; aa 341-543

Top scores:	**E-value**
Nuclear zinc finger protein *(C. elegans)*	e-122
CG1244 gene product [alt1, 2, 3, 4] *(Drosophila melanogaster)*	2e-10

E) ZK270.1 (983 aa)

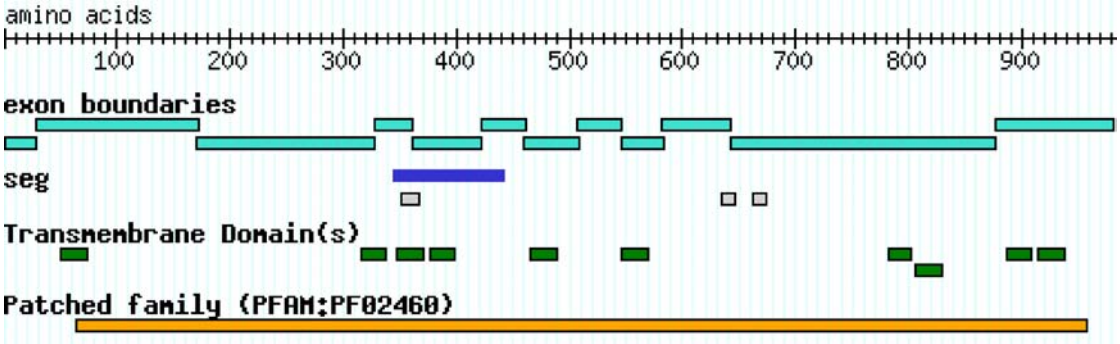

Protein BLAST with ZK270.1 - DAF-12 interaction region; aa 331-424

Top scores:	**E-value**
C. elegans PTR-12 protein	2e-18
C. elegans PTR-3 protein	2e-11
C. elegans hypothetical protein F44F4.4	4e-10

F) R144.7 (1065 aa)

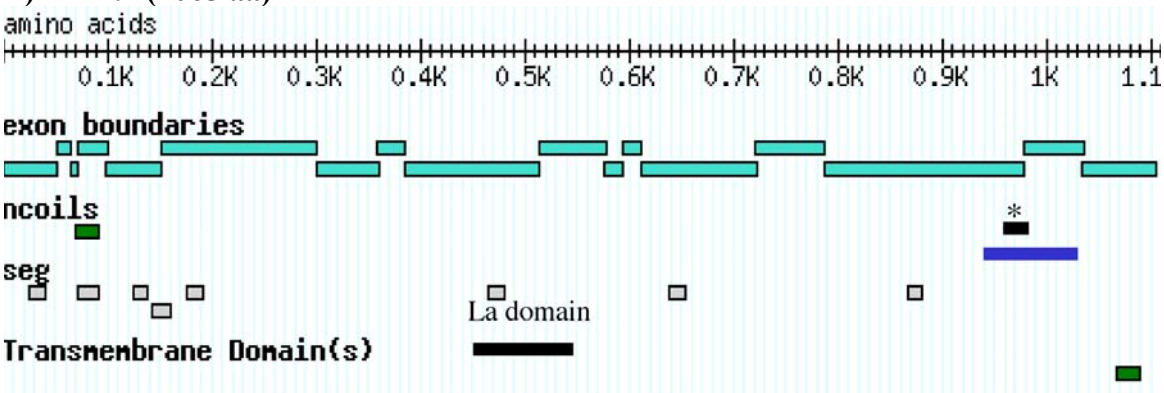

Protein BLAST with R144.7 - DAF-12 interaction region; aa 939-1028

Top scores:	**E-value**
KIAA0731 protein *(Homo sapiens)*	1e-23
La related protein *(Drosophila melanogaster)*	1e-22
Similar to RIKEN cDNA 3110040D16 gene *(Homo sapiens)*	2e-21

* conserved tandem domain of unknown function

937 NFNRNMYEEFRKLALEDAEIGS---RYGIEALFRFYSYGLEK 975

Figure 9) (This and previous page) Psort and BLAST analyses of putative DAF-12 interacting proteins isolated in the yeast-two hybrid screens I-IV. A) F46A11.2; **B)** M03F4.7; **C)** T05C1.6; **D)** M04B2.1; **E)** ZK270.1; **F)** R144.7. Light blue bars, predicted exon structure. Blue bars, DAF-12 interaction region. Green and grey bars, homology domains of unknown function. Orange bars, Pfam domains. Below, protein BLAST results, top scores with the DAF-12 interaction regions of the candidates; black bars in F) indicate La protein specific domains.

4.2 DIN-1, a putative DAF-12 cofactor

4.2.1 *din-1* structure

As a first functional approach to characterize the detected putative DAF-12 interacting proteins, we knocked down gene function by feeding worms with RNAi corresponding to our identified genes. In particular, F07A11.6 showed a previously undiscovered RNAi phenotype in *daf-12(rh61)* and other mutant backgrounds (see Part 4, this Chapter). In

addition, F07A11.6 had clear homologs in other species, the human SMRT/HDAC-associated repressor protein SHARP (Shi et al., 2001) and the *Drosophila* split ends protein SPEN (Rebay et al., 1999). Because of these features, we decided to focus our studies preferentially on this gene. We renamed it DIN-1, (DAF- 12 Interacting Protein 1). None of our other candidates had reproducible phenotypes including some genes with previously described RNAi phenotypes (Tables 5-8). Conceivably, the RNAi induction or fragment did not work effectively in all experiments.

Based on genefinder predictions, the largest product of DIN-1 consists of 2784 aa. *din-1* is located on the right arm of chromosome II, at position 11.7 (Figure 10). The *C. elegans* database (wormbase) predicts a *din-1* coding region spanning 18.3 kB that is organised in 21 exons. Two different splice variants are described, one that contains 21 exons and another isoform that lacks the exon 13 (Figure 10). The distance to the next upstream gene is 13 kb. Presumably, this region contains the *din-1* promoter.

4.2.2 *din-1* isoforms

When we analysed actual cDNAs, we discovered that the gene structure deviates from gene finder predictions. To determine the *din-1* molecular structure, we performed RT-PCR using the trans splice leader SL1 and reverse primers starting from exon 11 to obtain the 5'end, and oligo-dT and forward primers starting from exon 11 for the 3'end. We also

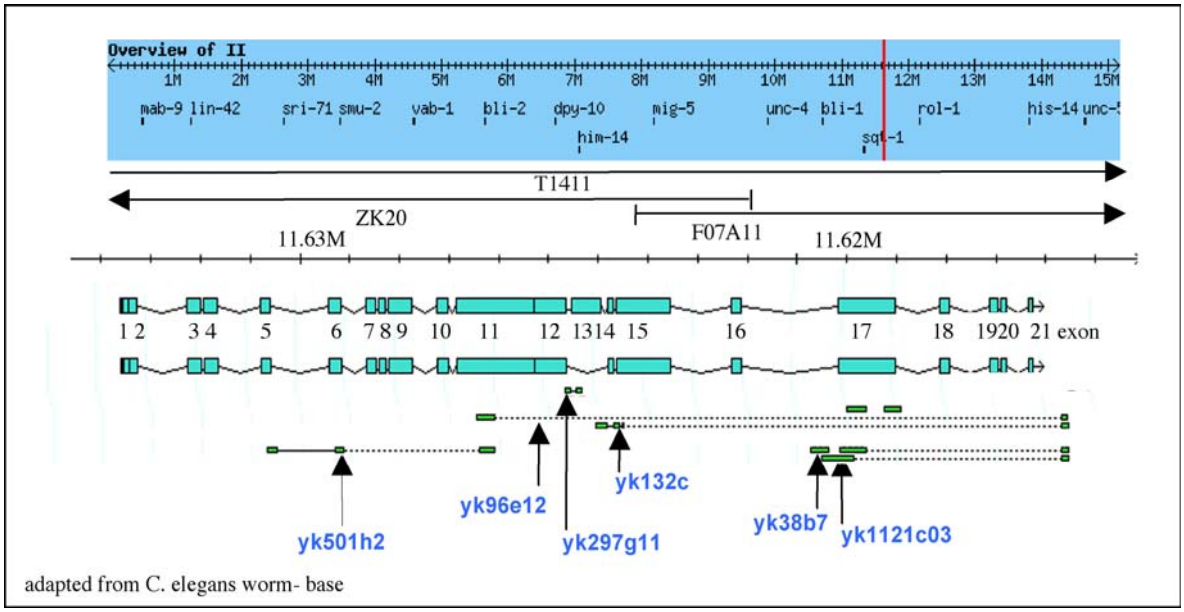

Figure 10) Genetic and physical structure of *din-1* locus. Upper panel, genetic map of the right arm of chromosome II. The position of *din-1* is indicated by the red line. Below this, cosmids covering the *din-1* region F07A11, T1411 and ZK20 are indicated as horizontal arrows. Lower panel, genomic structure of *din-1* predicted from wormbase. The EST clones sequenced for the determination of *din-1* structure are indicated with vertical arrows.

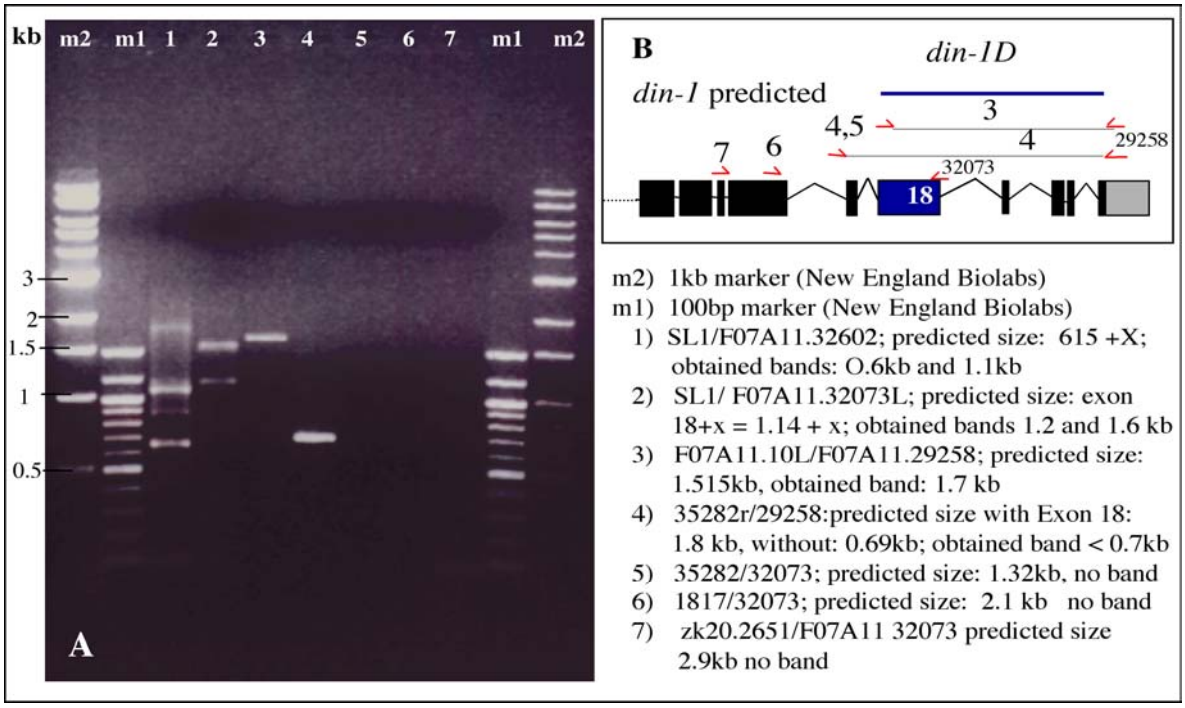

Figure 11) RT-PCR with SL1 and exon 18 specific primers. A) 1% agarose gel, RT-PCR products from *din-1* specific cDNA with primers listed below. **B)** Scheme of the localization of used primers according to predicted *din-1*. Primers are indicated (∠).

characterised *din-1* EST clones, provided by Y. Kohara (Table 9). Sequence analysis of the 5'end cDNA clones revealed an additional exon 3, not predicted by gene finder. We alsofound clones in which SL1 was spliced directly to exon 4, bypassing exons 1 2 and 3 (Table 9). When we analysed 3' end cDNA clones, we found that none of our isolated clones originating in exon 11 contained the predicted exon 18 (Table 9, Figure 11) nor did the YK clones 132c and yk96e12. However, we were able to amplify a PCR fragment from within the exon 18 to the *din-1* 3'end (Figure 11, lane 3). Moreover, the YK clones 38b7 and 1121c03 contain exon 18. These data suggest that the different 3'end clones result from alternate splicing and / or alternate promoter usage, giving rise to a short *din-1* isoform D. Consistent with the latter, when we performed RT-PCR with SL1 and two different exon 18 reverse primers, we obtained 2 PCR products, a 1.2 kb and a 1.7 kb fragment and a 0.6 and a 1.1 kb fragment, respectively (Figure 11, lane 1, 2). Sequencing revealed, that the 1.2 kb fragment in lane 2 contains SL1 spliced directly to the exon 18 5'end. Moreover, we failed to amplify the exon 18 when we were using primers in exon 17 and in the 3'UTR (in Figure 11, lane 4). We also did not obtain any PCR product when we used exon 18 reverse primers and exon 17 and 16 specific primers (Figure 11, lanes 5, 6, 7). In addition,sequence analyses reveals that YK clones 38b7 and 1121c03 begin in the intron upstream of Exon 18. Exon 18 contains a non-canonical splice acceptor CTTTAG, which

Table 9) Sequenced EST clones provided by Y. Kohara and sequenced cDNA clones from RT-PCR with N2 RNA; DIN-Isoform A

Exon number position according to cosmid	size of exon (bp)	size of upstream intron (bp)	Clones sequenced EST clone	cDNA clones
5'UTR 12080-12055				CKE5'-1, 2
1) ZK20 12055-11949	106	49		CKE5'-1
2) ZK20 11899-11733	167	50		CKE5'-1
3) ZK20 11682-11486	197	743		CKE5'-1
4) ZK20 10743-10472	270	76		CKE5'-1, 2
5) ZK20 10396-10126	271	854		CKE5'-1, 2
6) ZK20 9271-9057	215	1173	YK 501h2	CKE5'-1, 2
7) ZK20 7883-7638	246	513	YK 501h2	CKE5'-2
8) ZK20 7124-6935	190	48	YK 501h2	CKE5'-2
9) ZK20 6886-6733	154	56	YK 501h2	CKE5'-3
10) ZK20 6676-6199	478	502	YK 501h2	CKE5'-3
11) ZK20 5696-5487	210	149	YK 501h2	CKE5'-3
12) ZK20 5337-3790	1548	47	YK 501h2 YK 96e12	CKE3'-1
13) ZK20 3742-3098	645	105	YK 96e12 YK297g11	CKE3'-1
14) ZK20 2992-2405	588	139	YK 132c3 YK 297g11 YK 96e12	CKE3'-1
15) ZK20 2265-2158	108	64	YK 132	CKE3'-1
16) ZK20 1017-2093	1077	978	YK 132c3 YK 297g11 YK 96e12	CKE3'-1
17) F07A11 35192-35372	180	2858	YK 132c3 YK 297g11 YK 96e12	CKE3'-1
18) F07A11 31188-30999	190	816	YK 132c3 YK 96e12	CKE3'-1
19) F07A11 30182-30013	170	52	YK 132c3	CKE3'-1
20) F07A11 29960-29856	105	449	YK 132c3 YK 96 e12	CKE3'-1
21) F07A11 29406-29305	102		YK 96e12	CKE3'-1
3'UTR F07A11, 29103-28225 878bp			YK 132c3 YK 96e12	

Table 10) Sequenced EST clones provided by Y. Kohara and sequenced cDNA clones from RT-PCR with N2 RNA; DIN-Isoform D

Exon number position according to cosmid	size of exon (bp)	size of upstream intron (bp)	Clones sequenced EST clone	cDNA clones
1) F07A11 33215-32073	1143	884	YK 38b7	CKE18-1,2
2) F07A11 31188-30999	190	816	YK 132c3 VK 96e12	CKE3'-1
3) F07A11 30182-30013	170	52	YK 132c3 YK 96e12	CKE3'-1
4) F07A11 29961-29856	105	450	YK 132c3 YK 96e12	CKE3'-1
5) F07A11 29406-29302	104		YK 96e12	CKE3'-1
3'UTR F07A11 29103-28225	878		YK 132c3 YK 96e12	

deviates from the consensus splice acceptor TTTCAG. Other functional data supports the presence of the *din-1* isoform D (for details: see below).

In summary, *din-1* encodes at least 4 isoforms Figure 13. DIN-1 isoform A consists of 21 exons, it contains an additional exon 3 and lacks exon 18. SL1 is joined to the 5'UTR is at position bp12080 (ZK20), the position of poly A addition is at 28225 bp according to F07A11 (Table 9). It encodes a predicted protein of 2410 aa with a molecular weight of 267 kD (Figure 13A). DIN-1B lacks exon 13 and 18, it encodes a predicted protein of 2190 aa, with a molecular weight of 245 kDa. DIN-1C starts with exon 4 and lacks exon 18. It encodes a predicted protein of 2314 aa, with a molecular weight of 259 kDa. Finally, DIN-1D consists of exons 18-22, encoding a protein of 568 amino acids and its predicted weight is 61.3 kD.

4.2.3 DIN-1 homologs

To further characterize the predicted *din-1* gene products, we performed data base searches for functional domains and BLAST alignments. We found three DIN-1 homologs in other species, human SHARP (SMRT/HDAC associated repressor protein, Shi et al., 2001; Figure 14C), mouse MINT (MSX-2 interacting nuclear target protein, Newberry et al., 1999) and *Drosophila* SPEN (Split Ends, Rebay et al., 1999; Figure 14D). All of them are large nuclear proteins, SHARP contains 3349 aa, MINT contains 3567 aa and SPEN 5554 aa. All three proteins share at least two conserved domains, the N-terminal RNA recognition motives (RRMs), and a C- terminal conserved domain (Figure 14). In the RRMs, the homology between DIN-1 and homologs varies between 22% and 40%, in the C-terminal region, homology is between 27% and 28%.

We also found one *C. elegans* gene, F29C4.7 (Figure 14B), that contains the conserved C- and N-terminal domains. However, its overall architecture differs from the other DIN-1 homologs; it is shorter (529 aa), completely lacking the hinge region. The DIN-1 homology to F29C4.7 is 25% in the C-terminal domain and varies between 23% and 33% in the three RRMs.

4.2.4 DIN-1 functional domains

The largest region of DIN-1-DAF-12 interaction is found in isoform DIN-1D. It comprises the C-terminal domain only (Table 10, Figure 12, 14, 15). Ron Evans and co- workers have shown that SHARP acts as a corepressor by assembling components of the NuRD complex and HDACs (Evans et al., 2001). The C-terminal domain of SHARP directly interacts with

A) DIN-1 A, B, C

Isoform A 2410 aa; cDNA, 7176 bp; predicted molecular weight: 267 kD
Isoform B lacks exon 13; 2190 aa; cDNA, 6532 bp; predicted molecular weight: 245kDa
Isoform C lacks the exons 1+2; 2314 aa; cDNA, 6900 bp; starts with methionin at position 93 (M in blue); predicted molecular weight: 259kDa

```
   1  MVQVPSTNTV KESRHVAISG LPSTLPDDRL QLHFTKFGEI QRLVRQHGNP EIVLVSYM   60
  61  RGALRARSTK PQFEDSIEYK ISAYIPEPTQ  NSMASMSST PSSGQSSSPR NAELSPQRYG 120
 121  DTRGAEVKSP SFRNQMEARR GGGGPHLSVQ SQQRHSREYW SPIPEFPSES TACVVYEIQS 180
 181  GSTPERDLFE LVKKHSKRSG VPIDIQLEST TEPGWKKARV HYYRLDTDGL KADKSLILGR 240
 241  PPKFRVYYPT SGEQKHPQCH PSTSYAIPKL KGDHLLKASC SVHVPHLDRH SPDHYRRRFE 300
 301  SYGQVIDVDM VKSNDNKAFA VVQFTNIDDA QKALQDTNIP KPMSYQSRPS HRIIIFYLPI 360
 361  ECTNEEIMLI IRSLSDRIVD ICVDWWDRSA VITLDDMEPA NLLLKRMKLV GRNNFGEHKV 420
 421  AVDFCSDRFN LYFINRKKEN IEVAARSSSP TSKSENDQGS SSPSSSRDRQ NLHDPLQTRS 480
 481  SVEHHTNQED QENNASGSDS SSDSDSEEGS SSSNEDSDEQ NDVDEEDDED VVSEEKRHEP 540
 541  EEGKSSSPGN GHRDESNGDK DHEDSSERFS QPSTSSHHET SHSPEKDSEA YQSRSFSPLN 600
 601  YQSQSPGYEF LESKEIKQEF SPTTSSASSS DLELDMEMPD NPLTRMLERM HWRPFIDVSS 660
 661  FVNRIDEIVE LNQKARASYE KFTGRPFPKC NNDEVLSIQK IVFHEPRDYY YYENPCSELE 720
 721  VRIRDWRKLS DTADLDDFRA TDSKELGRDQ PAGGRTSGRP SLDESRTNRL SFDSTHHPAE 780
 781  LAQRSHSLCI GPMTPSTPFP TSQPLLVNTT HLPGTSQPST SGGITTPRSS QPPPLMSPVS 840
 841  RHNSMSSTGR PASIQTLRHQ SVMFPPDVSI PPPPIPPTHD EMMAPRGTPP SRRSSETMVP 900
 901  LRSPPFGTPI QNLLTMPIVP PPHLIAATST GTHSVSSSAH STPRHSISGT PVHCEPSNSK 960
 961  TSQPPTPKSR PEKVQIRHDT ISKSGPSNAI NALQARSQSM TSGDPKKSAP STPVVRDAG  1020
1081  EKERKKKEKE KEEREREARR EMKRKETKEE RNKRKEMERA KRLEDERQER KREKKKERDE 1140
1141  RKKEKEKVRK KAEKEKLKKK KHRKGDSSDE SDSDSNDELD LDVRKSTKEM TQEEKDHQLA 1200
1201  LLLSKGGIIE NLKSRRRSDK RAHDSFEKMQ QKSQQRRVLI ESSDDEGGKD GDKGNSSNGE 1260
1261  ESDSEKADLP PPPAPPSLSE SADQRLKVLK EREKGELTTS SDDEDHNDAG EIHQQRLTED 1320
1321  RENRKRQKSL TAYSSDEQGE RKNVPKRMRR DDSEDAAAKH PGWSAKDDQK QRKRKLEHRR 1380
1381  SSEDESKKNA KRDFRDIPHE DVSDEEETED GSRSRRQSTS STISNVTAKE RKEKSGKTPL 1440
1441  RIVPEPTGTP LLSPKILSPK HLSPKTSTSS TKRSSISDHE NLISPRQRNR TTSSTSTATT 1500
1501  SSKHEALSIP EKPLSPPVTA KSSVSSIDDP SIRDEFSMNS AADSPMSTTG RPMVLTKAAM 1560
1561  KAFNSTPPKK KNSSSGQHDS SSGSSSDSSS SDGSTSSDDS SDDEVPKQTE PVTSIPVVAS 1620
1621  DNGSPENVVV ETPSIVSQTP REPEPFTISE QSSESEPEAV PECPEASVEP QMETSQNVEP 1680
1681  VSEEHEDSHE HGDSEVAVES QQQPLEHQEE KEELENKILD VAAEHHEEQV QGDEDSVESS 1740
1741  IPAPSDEPDP VTQAQEKSAH TLISDQETDQ AVQSIFDEEE ADEFPQYPDF GISTNEKEV  1800
1801  GKDPHNIKPT EPLNNGHTDL LFSPSSSAHA SEKQSTKSED DMEEDSELVV MEKEVPMEQV 1860
1861  IAQEVHVPSE PSPMEEEVKL ETSPVPKEEP IKMEESPEQT PTPDLISNNE SQDTPGAVNN 1920
1921  HLHENHDAVQ TPIQLQPASQ HQVAQPSPRP AVAPDSQQNG PVLVSQQSQP SPMSSQQSDM 1980
1981  AQNLILSSKD INDLAAKLHK NPEALAQATR GDCSGIFQHL LLHAQGNGQN MTPEMLQLK  2040
2041  AFFAQQQENE ANQMMQAKMK QQTINKDRIK EQERVKRMYE ENERKVEEDR REKQRKEEER 2100
2101  QRLAAATAAA TMATQKAAEA LKQKQEVPRH GFQHVLSMMT PEARSLYEQF PGLSSYINRD 2160
2161  SIGATNGVLH LPTQSIQRPS STASTSSNPP KAPLQPSASV NQNTIDPAEI EEIRVQRWF  2220
2221  KHFPMVWTGR LALKSTEAMI NLHLINGSET FLNDVLGRQV TEENPRRDSV KILQRLRLDN 2280
2281  GQVEHIYRIL TNPEYACCLA LSSVNNIENL KENDTNLKSH FIDYLINKKI AGISSLGEVE 2340
2341  TKFKSARVHV FAPGEIVNRY LSELATSLHD YLQNTDTRYL LIVFTNDKAD PNMTGPPSVA 2400
2401  SLAVPPVSST                                                       2410
```

B) DIN-1D

568 aa, genomic; cDNA size; 1.7 kb
Predictet weight: 61.337 kD
Protein sequence:

```
                        dh149                          dh127
   1  MSAEEAATVM AVASSDPNPP ATSTVDLAAM LQQLQAAQAA QAAQQVPVVT TASTPNPLSN  60
                                                                dh181
  61  LETLLSTASL ANLATGGALN PLSMLALTSS LNQSSPVYQG IARVLLTMNM GQMLATHQTS 120
 121  ELLATMNQQE TLMALLAARN GLPFAMPQQN QQPQMPAQGG FAIPTVLPHM SLKRNAKDQL 180
 181  SVGGVSDRKK SCPLHAMIGQ GQQPPPPQQP MQAVAPAPPR SPSPPRKSMF ENLPPEMKEK 240
 241  NEMFRKEILR RLDIILLEEL GAEDEEDQKP DLKQIPTSEE DTDDSKADSM GAEGSAFRRI 300
        dh118,dh128
 301  LSRSSTMGNN SGSPSASGTT SPSTSSSISS GPDSPPLEGE PLNSEFMDML TEVAQKHREQ 360
 361  SNTDALSAKI VDEQSFSQHF PMVWTGRLAL KSTEAMINLH LINGSETFLN DVLGRQVTEE 420
 421  NPRRDSVKIL QRLRLDNGQV EHIYRILTNP EYACCLALSS VNNIENLKEN DTNLKSHFID 480
 481  YLINKKIAGI SSLGEVETKF KSARVHVFAP GEIVNRYLSE LATSLHDYLQ NTDTRYLLIV 540
 541  FTNDKADPNM TGPPSVASLA VPPVSST                                    568
```

A) RNA recogniton motifs in green
NLS = Nuclear Localization Site cluster in red
underlined black: L/IXXL/IL/I (Rosenfeld et al., 2001; aa 368, 2285)
corepressor motifs
underlined red: LxxLL coactivator motif (aa1198)
DIN-1-DAF-12 interaction domain in blue
Exons 1+2 in bold
Exon 13 in italics
Exon 3 in purple
Consensus Akt/PKB phosphorylation site, RXRXXS/T(hyd) (Alessi et al.,1996) aa 295, 1324, 1413 and 1485 in purple
DIN-1 N- terminal epitopic Antibody in light green (aa 558-578)

B) underlined black: corepressor motifs
I/LXXI/VI (Hu et al) (aa408)
L/IXXL/IL/I (aa252, 442)
underlined red: LxxLL coactivator motifs (aa61,132)
DIN-1-DAF-12 interaction domain in blue (aa 21- 568)
H: end exon 18
DIN-1 C-terminal epitopic Antibody in light green (aa 278- 290)
underlied, italics: *din-1* mutants

Figure 12) DIN-1 protein sequence, functional domains. A) DIN-1 isoform A, B and C based on sequence analyses of cDNAs and YK clones; **B)** DIN-1 isoform D.

SMRT and components of the NurD complex. We assume that the C- terminal domain in DIN-1 has a similar function.

In *DIN-1D*, we identified three consensus L/IXXL/IL/I motifs and related motifs (Hu et al., 2001; Rosenfeld et al., 2001, underlined and bold in Figure 12B) and another three similar motifs (underlined in Figure 12B). These domains are typical of nuclear hormone receptor corepressors, like N-CoR (Kurokawa, 1995) or SMRT (Chen and Evans, 1995). They are also present in the receptor interaction domain of SHARP (Figure 14). DIN-1A, B and C contain two L/IXXL/IL/I-like motifs (Figure 12A). Altogether, these data suggest that DIN-1 might function as corepressor.

DIN-1 also contains LXXLL motifs that are characteristic for nuclear receptor coactivators. DIN-1D contains two such motifs within the exon 18, indicating that it might also have anactivation function. In isoforms A, B, C, there is one LXXLL motif (Figure 12). Remarkably, SHARP interacts with the RNA coactivator SRA through its four conserved RNA recognition motifs. At least three RRMs are also present in DIN-1, (Figure 12A, 14), providing a target for regulative RNAs also in DIN-1.

The DIN-1 isoforms A and C contain four consensus Akt/PKB RXRXXS/T phospho rylation sites (Alessi et al., 1996; aa 295, 1324, 1413 and 1485 according to DIN-1A (Figure 12A), indicating that DIN-1 might be a target of kinases like AKT-1 and AKT-2. Two out of four of these motifs are localized in exon13, thus they are not contained in DIN-1 isoform B.

DIN-1 contains 23 nuclear localization sites (NLS) detected by Psort in the middle of the protein, clustering at position 1084-1171 and 1371-1395 (Figures 12, 14, 15), consistent with a function in the nucleus.

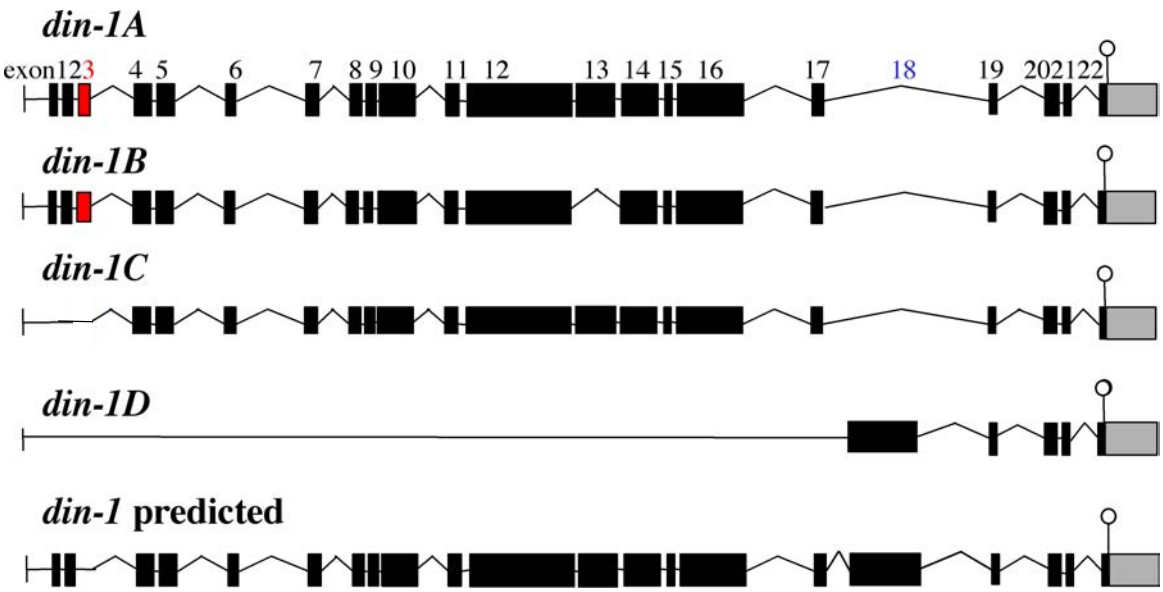

Figure 13) Splice variants of *din-1*. *din-1A* comprises the exons 1-22, and lacks exon 18. Isoforms A, B and C have an additional exon 3 (red). *din-1B* lacks exon 13 and 18, *din-1C* lacks exons 1,2 and 18. *din-1D* is composed of exons 18-22, stop codon, dash and arrow. The isoforms A, C and D were compiled by sequence analyses of EST clones provided by Y. Kohara as well as cDNA obtained from RT-PCR (Table 9). Isoform B is based on sequencing data from YK clones yk501h2, yk96e12, yk297g11 and yk132c3.

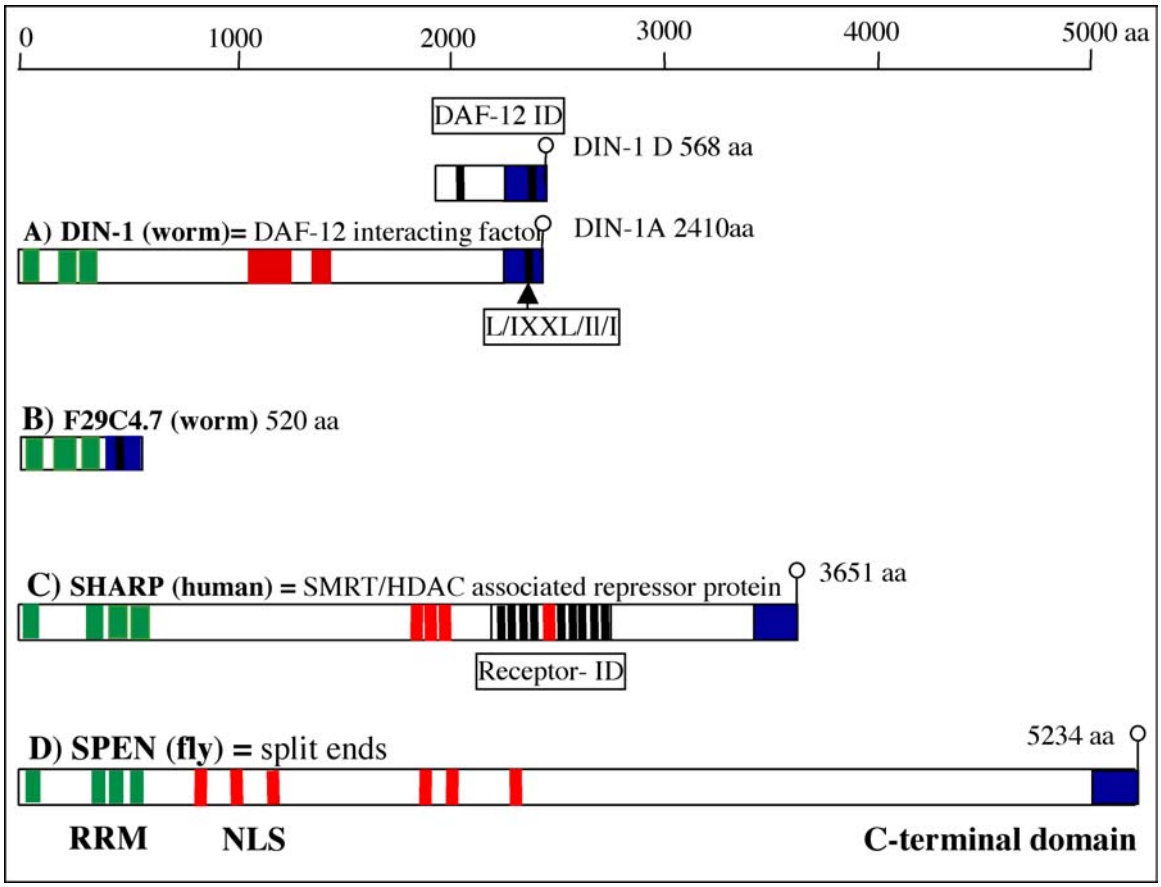

Figure 14) Domain structure of DIN-1 and homologs. A) C. elegans DIN-1, **B)** *C. elegans* F29C4.7, **C)** *Homo sapiens* SHARP, **D)** *Drosophila melanogaster* Spen**.** C-terminal domain in blue; RRM=RNA recognition motif in green; NLS= Nuclear localization sites in red. The homology of the DIN-1 C-terminal domain to SHARP and SPEN is 28%. The DIN-1 RRM homology with SHARP is 40%. The DIN-1 region of interaction with DAF-12 (DAF-12 ID) and the SHARP receptor interaction domain are indicated in black boxes. 3 L/IXXL/I corepressor motifs are found in DIN-1, 9 in the receptor-ID of SHARP (black bars).

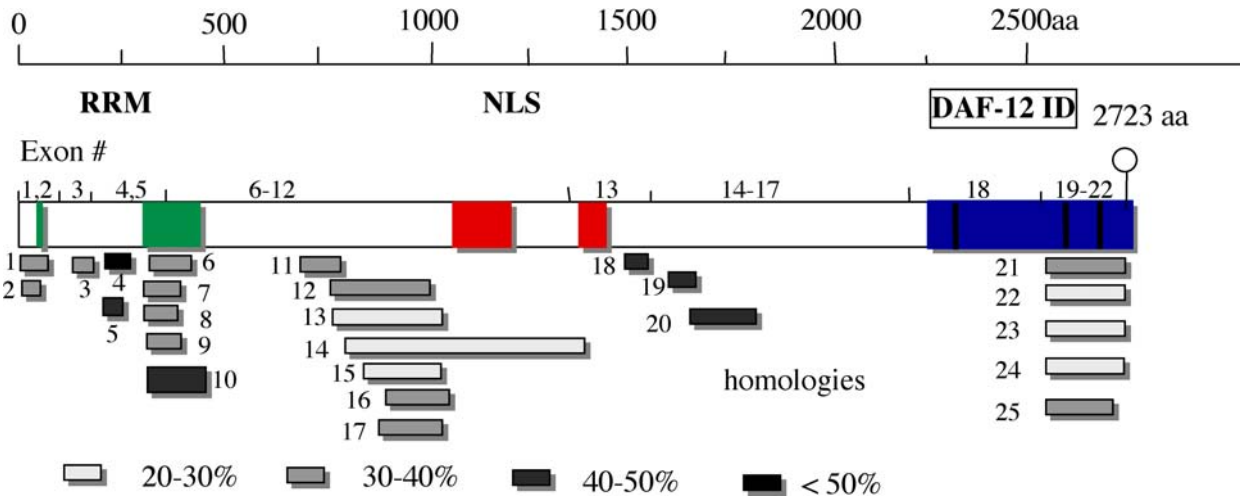

Figure 15) Predicted DIN-1 structure and functional domains. Protein BLAST alignments of different DIN-1 domains. Green boxes: RNA recognition motifs, red boxes: cluster of nuclear localization sites, blue box: C-terminal domain with L/IXXL/I motifs (black bars). Underneath are listed the top homologies from the protein BLAST searches.

Exon 1+2 aa 1-92

1) Similar to Putative RNA-binding protein 15 (RNA binding motif protein 15)(One-twenty two protein) *(Homo sapiens*) Identities = 23/69 **(33%)**, Positives = 34/69 (48%) aa 6-70
2) ELAV protein (Embryonic lethal abnormal visual protein) *(Drosophila)* Identities =16/47 **(34%),** aa 5-49

Exon 3 aa 93-142

3) 1 hit only: complement component C3-4 *(Oncorhynchus mykiss)* Identities = 15/42 **(35%),** Positives = 21/42, (49%) aa110-153

Exon 4+5 aa 143-322

4) Heat shock protein 90 *(Paramecium tetraurelia*) Identities = 15/28 **(53%),** Positives = 22/28 (78%) aa 160-198
5) ADIR2 *(Homo sapiens)* Expect = 2.1 Identities = 17/39 **(43%),** Positives = 25/39 (63%), aa185-212
6) Hypothetical protein Y55F3AM.3a *(C. elegans),* RRM, Identities = 17/42 **(40%),** Positives = 29/42 (68%),
aa 299-338
7) PR264/SC35 *(Mus musculus)* Identities = 20/49 **(40%)**, Positives = 31/49 (62%) aa 289-334
8) Similar to splicing factor, arginine/serine-rich 2 (SC-35) *(Homo sapiens)* Identities = 20/49 **(40%),** = 31/49 (62%), 289-334
9) Cold-inducible RNA-binding protein (Glycine-rich RNA-binding protein CIRP) (A18 hnRNP), Identities = 17/43 **(39%),** Positives = 25/43 (57%) aa 299-338
10) SHRP RRM, based on protein alignment (40%)(Kuang et al, 2000)

Exon 6-12 aa 323-1337

11) Similar to Dystrophia myotonica-containing WD repeat motif protein (DMR-N9 protein) *(Homo sapiens);* Identities = 41/125 **(32%),** Positives = 60/125 (47%); aa 739-784
12) Tubby super-family protein *(Mus musculus)* Identities = 49/207 **(23%),** Positives =79/207 (37%), aa 774-977
13) F11A1.3 -DAF-12; *(C. elegans);* Identities = 53/231 **(22%),** Positives = 81/231 (34%), aa 777-1003
14) Mucin and cadherin-like; mu-protocadherin *(Rattus norvegicus)* Identities = 56/212 **(26%),** Positives = 81/212 (37%), aa 794-1341
15) Putative protein kinase APK1A *(Arabidopsis thaliana)* Identities =45/169 **(26%),** Positives =55/169 (31%), aa 821-974
16) Hypothetical protein F46C3.3 (*C. elegans)* hum-4; ATP binding, actin binding; Identities = 35/116 **(30%),** Positives = 46/116 (39%) aa 888-1002
17) Ankyrin-B; *(Homo sapiens)* Identities = 51/199 **(25%),** Positives = 74/199 (36%), aa 797-997

Exon 13 aa 1338-1551

18) Voltage-gated Na channel NaCh6 (*Rattus norvegicus*); Identities = 20/42 **(47%),** Positives = 23/42, (54%); aa 1533-1574

Exon 14-17 aa 1552-2202

19) Titin, isoform N2-A; connectin; CMH9, included *(Homo sapiens),* Identities = 27/66 **(40%),** Positives =31/66 **(46%),** aa 1606-1670
20) Synapse-associated protein 97 *(Rattus norvegicus)*=drosophila discs-large tumor suppressor homolog, Length= 911 Score = 33.1 bits (74), Identities = 15/36 **(41%),** Positives = 22/36 (60%), aa 1662-1803

Exon 18 aa 2202-2565 no homologies

Exon 19-22 aa 2566-2723

21) dJ134O19.4 (novel protein) *(Homo sapiens)* Identities = 54/191 **(28%),** Positives = 94/191 (48%), aa 2547-
2729, in protein: 70-255; not sharp!
22) Msx-2 interacting nuclear target protein *(Mus musculus),* Identities = 53/190 **(27%),** Positives =94/190 (48%),aa 2567-2729 in protein: 3364-3548
23) SHARP; 2567-2729 (din-1); 3476-3661
24) Spen gene product *(Drosophila melanogaster),* identities = 46/164 **(28%),** Positives = 84/164(51%), aa 2567-2729, Spen 5371-5529
25) Similar to Putative RNA-binding protein 15 (RNA binding motif protein 15) (One-twenty two protein) *(Homo sapiens),* Identities = 51/217 **(23%),** Positives = 98/217 (44%), aa 2575-2722prot 683-89

To gain a better insight into the functional domain structure of DIN-1, we performed protein BLAST alignments with seven segments of the protein (Figure 15). Exons 1 and 2 show 33% homology to RNA Recognition motifs (1 in Figure 15), exons 4+5 showed 53% homology to heat shock protein 90 from *Paramecium tetraurelia* (4 in Figure 15). In this region, there is 40% homology with SHARP RRM (10 in Figure15). Exon 13 has 47% homology with a mammalian voltage gated Na^+ channel (18 in Figure15). Remarkably, exon 18 had no homologs at all. In the exon 19-22 we found homologies to SHARP (23), MINT (both 27%) (22), SPEN (28%)(24 in Figure 15) and human One twenty two protein (25).

4.3 DIN-1 DAF-12 interaction domain

We originally detected DIN-1 as a DAF-12 interacting factor in the yeast-two hybrid system using a bait construct that contained the DAF-12 hinge- and LBD (Figure 7B, 16A). When we tested the two long DAF-12 isoforms A1 and A3 for interaction with DIN-1, we observed an activation of the two-hybrid reporter genes Leu-2 and His-3 by DAF-12A3, but not by DAF-12A1 (Figure 16A). We suspect that this result is due to a low expression level of DAF-12A1 rather than a missing physiological interaction between DAF-12A1 and DIN-1. In a westernbut we got a signal with LexA alone (data not shown). Moreover, when we used DAF-12A1 as bait in the yeast- two hybrid screens, the total numbers of positive clones was 70 fold reducedblot assay with antibodies directed against LexA we could not detect DAF-12A1

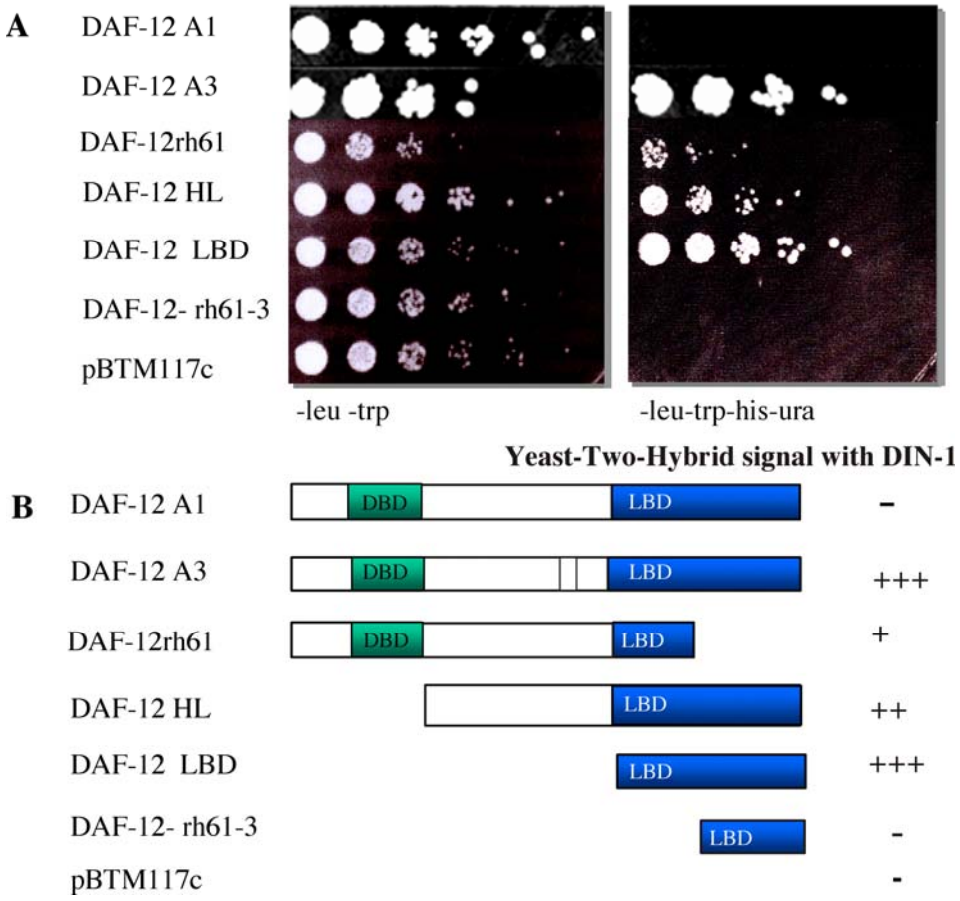

Figure 16) Minimal DAF-12 / DIN-1 interaction domain. DIN-1 gives a two- hybrid signal with the DAF-12 isoform A3 but not with the isoform A1. **A)** Dilution series of the yeast strain L40ccu-pACT-31DIN-1 transformed with and pBTM117cDAF-12A1, pBTM117cDAF-12A3, pBTM117cDAF-12rh61, pBTM117cDAF-12HL, pBTM117cDAF-12LBD, pBTM117cDAF-12rh61-3 and pBTM 117c. Left panel: Growth on SD medium-leu -trp, right panel, growth on SD medium -leu -trp -ura -his. **B)** Scheme of the used bait proteins DAF-12A1 DAF-12A3, DAF-12 rh61, DAF-12HL, DAF-12LBD and DAF-12rh61-3.

expression, in comparison to DAF-12 A3 as bait. Finally, in Screen I, we used a bait containing the C-terminal part of DAF-12A1 that was expressed abundantly.

To further define the minimal interaction region between DAF-12 and DIN-1, we tested several DAF-12 constructs (Figure 16B). A truncated version of DAF-12, lacking the very C-terminal region interacts with DIN-1 (Daf-12rh61 in Figure 16B) as well as DAF-12 LBD, which contains the LBD only (Daf-12 LBD in Figure 16B) and Daf-12H, expressing the LBD and hinge region only (data not shown).

However, the interaction was disrupted when we further truncated the DAF-12 LBD, indicating that the region between aa 1503 and 1881 within the LBD is crucial for the interaction between DAF-12 and DIN-1. Interestingly this region corresponds to the helixes H1-H6 within the DAF-12 LBD that is critical for the nuclear hormone receptor corepressor interaction (Hu, 1999; Perissi, 1999). However, these results need to be confirmed by testing the protein stability in a western blot against a lexA antibody.

4.4 *din-1* RNAi phenotypes

We next examined *din-1* phenotypes. To do this we performed RNAi feeding assays using a *din-1* fragment obtained from the yeast-two hybrid screen (clone 32415-33144, Table 5). We scored wild type hermaphrodites and several dauer pathways mutants of all stages grown at different temperature for phenotypic abnormalities, including formation of adult alae, dauer formation, seam cell development, and gonadal development and migration.

Animals fed *din-1RNAi* have no obvious phenotype on their own. However, we found that *din-1RNAi* was a potent suppresser of several Daf-c mutants from insulin/IGF, TGF-ß, and cGMP pathways (Figure 17). At 25°C, *daf-2(e1368)* insulin receptor class I mutants form 82% dauer larvae, a phenotype suppressed by *din-1RNAi*, displaying only 2% dauer phenotype (Figure 17A). 99.5% of *daf-2(m41)* mutants, another insulin receptor class I allele, which form dauers under same conditions, is suppressed by *din-1RNAi* by 56.5% (Figure 17B). In contrast, *din-1RNAi* could not suppress the Daf-c phenotype of the class II *daf-2* allele (*e1370)*: Under reproductive conditions, 99% of the mutants formed dauers and 92% of *din-1RNAi* treated animals went into dauer as well (Figure 17C).

Similarly, the Daf-c phenotypes of *daf-7(e1372)* (TGF- ß pathway) and *daf-11(m47)* (cGMP pathway) mutants are suppressed by *din-1RNAi*. 78% *daf-7(e1372)* worms formed dauer at

25°C, whereas only 3% of *daf-7(e1372)* animals grown on *din-1RNAi* formed dauer larvae under the same conditions (Figure 17D). 91% *daf-11(m47)* mutants formed dauer, but only 14% *daf-11(m47;/din-1 RNAi* (Figure 17E).

We next performed genetic epistasis experiments on Daf-c mutants further downstream in the dauer pathways (Figure 18). *din-1RNAi* suppressed the Daf-c phenotype of the *daf-12* LBD allele *rh273*, 18% of the mutants formed dauer larvae whereas no dauers were formed with *din-1RNAi* (Figure 18A). Together, these data suggest that *din-1* acts downstream of hormone binding to DAF-12. We also found that *din-1* was a potent suppressor of the heterochronic phenotypes seen in some *daf-9* and *daf-12* alleles (Figure 18C, D). The *daf-12*(*rh61)* LBD mutants as well *daf-9(rh50)* display gonadal Mig phenotypes, interpreted as a heterochronic delay in stage specific migrations.

In Figure 19, we documented the gonadal Mig phenotype of *daf-12*(*rh61)*: In contrast to wild type (Figure 19A) the mutant gonad does not undergo reflection at all (Figure 19C). The gonadal Mig phenotype is suppressed by *din-1RNAi*: 87% of *daf-9(rh50)* animals showed the gonadal Mig- phenotype on L4440, but only 16% of *daf-9(rh50)* grown on *din-1RNAi* plates (Figure 18B). 99.5% of the scored *daf-12(rh61)* worms showed the gonadal Mig phenotype, but only 0.5% of the *daf-12(rh61) din-1 RNAi* animals (Figure 18D, 19B).

The suppression of the gonadal Mig phenotype is not complete. Whereas the gonad of wild type animals reflexes half way back towards the vulva (Figure 19A), the gonad of *daf-12(rh61) din-1RNAi* animals of the same age is reflexed, but not to the same extent (Figure 19B). Another heterochronic phenotype, the adult alae, disrupts the formation of cuticular lateral ridges. In addition to the Mig phenotype, the heterochronic alae gap phenotype of *daf-12(rh61)* adults is suppressed by *din-1RNAi* (Figure 19 D, E, F). In wild type there is continuous alae (Figure 19D), whereas in *daf-12(rh61)* animals, the alae has several gaps of different sizes (Figure 19F). In *daf-12(rh61) din-1RNAi* worms the wildtype situation of a continuous alae is restored (Figure 19E).

dre-1 is a mutant that was isolated as an enhancer of *daf-12* null mutant gonadal Mig phenotype. When we grew *dre-1* worms on plates with *din-1 RNAi*, we observed an enhancement of the gonadal Mig phenotype (data not shown) suggesting that *dre-1* and *din-1* act in the same pathway.

Ron Evans and coworkers have shown that the DIN-1 homolog SHARP interacts with HDACs and other members of the Nurd complex via its C- terminal do- main. In *C. elegans,*

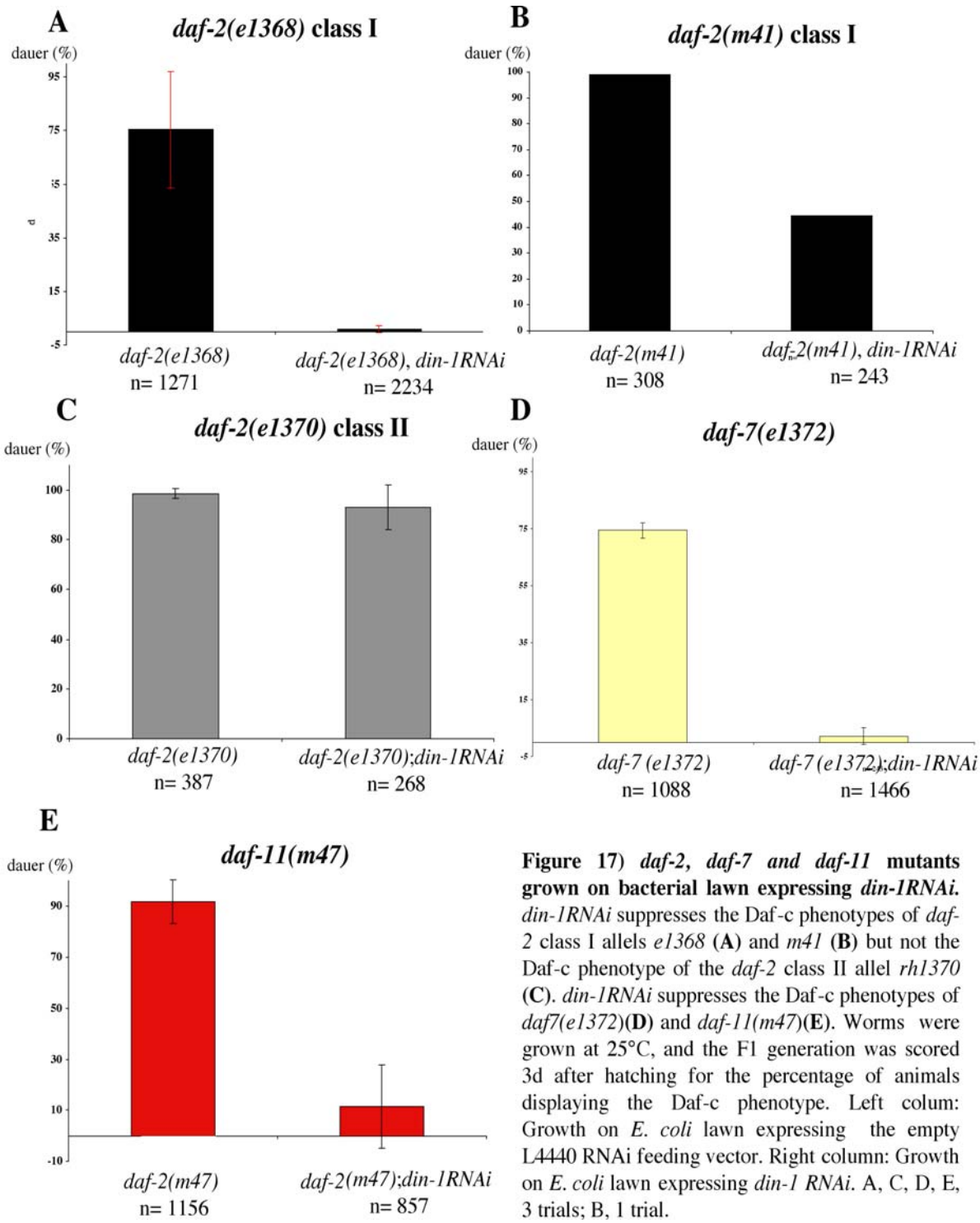

Figure 17) *daf-2, daf-7 and daf-11* mutants grown on bacterial lawn expressing *din-1RNAi.* *din-1RNAi* suppresses the Daf-c phenotypes of *daf-2* class I allels *e1368* (**A**) and *m41* (**B**) but not the Daf-c phenotype of the *daf-2* class II allel *rh1370* (**C**). *din-1RNAi* suppresses the Daf-c phenotypes of *daf7(e1372)*(**D**) and *daf-11(m47)*(**E**). Worms were grown at 25°C, and the F1 generation was scored 3d after hatching for the percentage of animals displaying the Daf-c phenotype. Left colum: Growth on *E. coli* lawn expressing the empty L4440 RNAi feeding vector. Right column: Growth on *E. coli* lawn expressing *din-1 RNAi*. A, C, D, E, 3 trials; B, 1 trial.

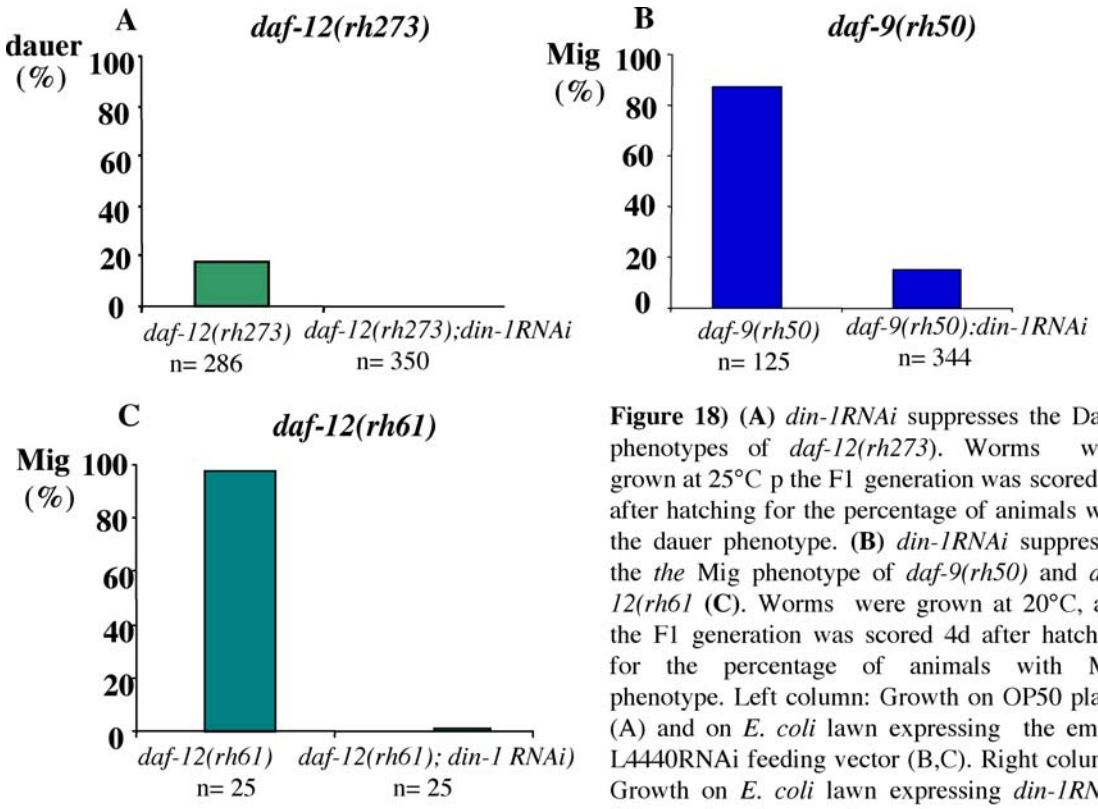

Figure 18) (A) *din-1RNAi* suppresses the Daf-c phenotypes of *daf-12(rh273)*. Worms were grown at 25°C p the F1 generation was scored 3d after hatching for the percentage of animals with the dauer phenotype. **(B)** *din-1RNAi* suppresses the *the* Mig phenotype of *daf-9(rh50)* and *daf-12(rh61* **(C)**. Worms were grown at 20°C, and the F1 generation was scored 4d after hatching for the percentage of animals with Mig phenotype. Left column: Growth on OP50 plates (A) and on *E. coli* lawn expressing the empty L4440RNAi feeding vector (B,C). Right column: Growth on *E. coli* lawn expressing *din-1RNAi*. All experiments were done only once

there are several homologs of HDACs and Nurd complex genes. To test if there is genetic connection between these genes and *din-1* or Daf-genes, we performed RNAi feeding assays. We grew N2, *daf-12(rh61), daf-2(e1368), daf-2(e1370), din-1(dh127); daf-2(e1370)* on plates expressing RNAi against HDACs, corepressors and Nurd complex genes. We scored the progeny for various phenotypes, including enhancement or repression of the Mig or Daf-cphenotypes (Table 11). Several *C. elegans* HDACs and Nurd complex genes were provided in a chromosome I RNAi feeding vector library by J. Ahringer: R06C1.1 (HDAC), F02E9.4 (*pqn-28*, putative SIN-3 ortholog), B0025.3 (Alien), C32F10.2 (*lin-35*, retinoblastoma associated protein), C32F10.4, K07A11.11 (*rba-1* Retinoblast binding protein, RBAP 46 like),K07A1.12 (*lin-53*), *hda-1, hda-2* (putative HDAC1, 2 orthologs) and C26C6.5 (p66 subunit in the NuRD complex). For some of the tested genes, phenotypes have been described previously, B0025.3 has defects in gonadal formation resulting in short gonad arms and sterility, K07A1.11 and K07A1.12 are reported to be embryonic lethal. C26C6.5 displays a Mig and protruding vulva phenotype (Ahringer, 2000). These phenotypes could be confirmed. For R06C1.1 and C32F10.4 we did not observe any changes of phenotype in all scored

Table 11) RNAi experiments with HDA-complex components

a) R06C1.1 RNAi; histone-deacetylase

Genotypes	**20°**	**25°**	**RNAi 20°**	**RNAi 25°**
N2	Normal	Normal	Normal	Normal
daf-12(rh61)	Mig	Mig	Mig	Mig
daf-2(e1368)	Non-Daf	Daf-c	Non-Daf	329 non-Daf : 201 Daf-c, partial suppression
daf-2(e1370)	Non-Daf	Daf-c	Non-Daf	Daf-c

b) F02E9.4 (*pqn-28*) RNAi; putative *sin-3* Ortholog in *C. elegans*

Genotypes	**20°**	**25°**	**RNAi 20°**	**RNAi 25°**
N2	Normal	Normal	Normal	Normal
daf-12(rh61)	Mig	Mig	Mig	Weak suppression,grow slowly
daf-2(e1368)	Non-Daf	Daf-c	Non-Daf	Daf-c
daf-2(e1370)	Non-Daf	Daf-c	Non-Daf	Daf-c

c) B0025.3RNAi; Alien by Ahringer JA et al: 50-80% embryonic lethality

Genotypes	**20°**	**25°**	**RNAi 20°**	**RNAi 25°**
N2	Normal	Normal	Normal	Defects in gonadal formation (Mig), short gonadal arms, steril
daf-12(rh61)	Mig	Mig	Mig	No suppression, steril
daf-2 (e1368)	Non-daf	Daf-c	Non-Daf	Daf-c
daf-2(e1370)	Non-daf	Daf-c	Non-daf	Daf-c

d) C32F10.2 (*lin-35*) RNAi; homolog to retinoblastoma-associated protein

Genotypes	**20°**	**25°**	**RNAi 20°**	**RNAi 25°**
N2	Normal	Normal	Normal	Sick, thin, lighter
daf-12(rh61)	Mig	Mig	Mig	Weak suppression
daf-2(e1368), daf-2(e1370)	Non-Daf	Daf-c	Non-Daf	Daf-c
daf-2 (e1370);din-1(36-1)	Non-Daf	Daf-c	Non-Daf	Daf-c

e) C32F10.4 RNAi

Genotypes	**20°**	**25°**	**RNAi 20°**	**RNAi 25°**
N2	Normal	Normal	Normal	Normal
daf-12(rh61)	Mig	Mig	Mig	Mig
daf-2(e1368), daf-2(e1370)	Non-daf	Daf-c	Non-daf	Daf-c

f) K07A1.11RNAi; *rba-1,* Retinoblast binding protein RBAP 46 like

Genotypes	**20°**	**25°**	**RNAi 20°**	**RNAi 25°**
N2	Normal	Normal	embryonic lethal	embryonic lethal
daf-2(e1368)	Non-daf	Daf-c	Non-Daf	Daf-c
daf-2(e1370)	Non-daf	Daf-c	Non-daf	Daf-c

g) K07A1.12 (*lin-53)*RNAi

Genotypes	**20°**	**25°**	**RNAi 20°**	**RNAi 25°**
N2	Normal	Normal	embryonic lethal	embryonic lethal
daf-2(e1368)	Non-daf	Daf-c	Non-Daf	Daf-c
daf-2(e1370)	Non-daf	Daf-c	Non-daf	Daf-c

h) *hda-1, hda-2*RNAi; putative orthologue of HDAC-1, HDAC-2

Genotypes	**20°**	**25°**	**RNAi 20°**	**RNAi 25°**
N2	Normal	Normal	Normal	Normal
daf-12(rh61)	Mig	Mig	Mig	Mig
daf-2(e1368)	Non-daf	Daf-c	Non-daf	Daf-c
daf-2(e1370)	Non-daf	Daf-c	Non-Daf	Daf-c
daf-2(1370); din-1(dh127)	Non-daf	Daf-c	Non-Daf	Daf-c

i) C26C6.5 RNAi; p66 subunit in the NuRD complex

Genotypes	**20°**	**25°**	**RNAi 20°**	**RNAi 25°**
N2	Normal	Normal	weak Mig	Mig, sick, protruding vulva
daf-12(rh61)	Mig	Mig	Mig	Mig
daf-2(e1368)	Non-daf	Daf-c	Non-daf	Daf-c
daf-2(e1370)	Non-Daf	Daf-c	Non-Daf	Daf-c

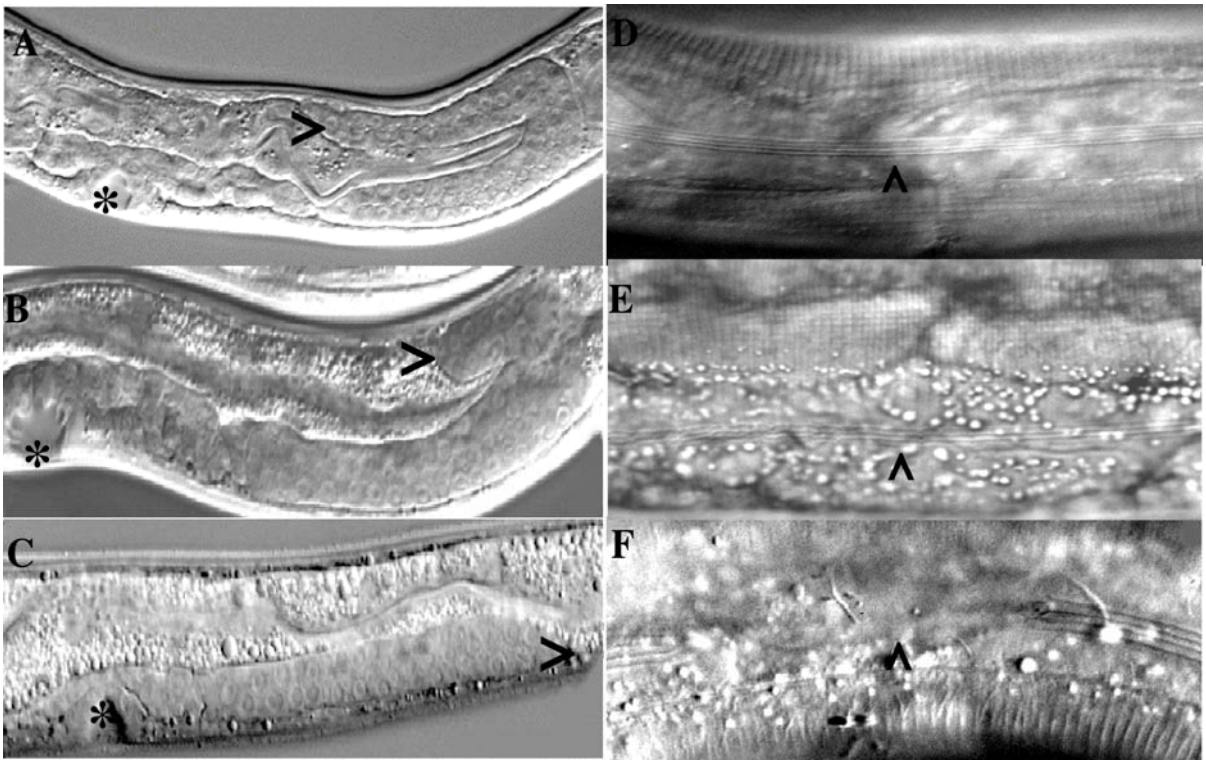

Figure 19) *din-1RNAi* suppresses the *daf-12(rh61)* Mig and alae gap phenotype. N2 **(A, D)** and *daf-12(rh61)* **(B, C, E, F)** worms were grown on a bacterial lawn expressing the RNAi feeding vector L4440 **(A, C, D, F)** or *din-1RNAi* (**B, E)**. The F1 generation was scored for gonadal phenotypes at L4 stage after 2d of growth at 20°C **(A, B, C)**; adults were scored after 4d of growth for alae phenotypes at 20°C **(D, E, F)**. Left panel: Vulva (*), gonadal arm and distal tip cell (arrowhead). Right panel: Adult alae and alae gaps are indicated with an arrowhead. Left lateral aspect, **A, B, C**, at 63x; **D, E, F** 100x magnification.

animals, F02E9.4 and C3 2F10.2 caused a very weak suppression of the *daf-12(rh61)* Mig phenotype, N2 worms grown C32F10.2 plates looked thinner and lighter compared to control animals. Under these conditions, we could not establish a clear connection between the tested HDACs and Nurd complex genes and the tested mutants on a genetic level.

4.5 DIN-1 mutants

4.5.1 Isolation of *din-1* alleles

In order to isolate stable *din-1* alleles, we screened for revertants of the *daf-12(rh61)* gonadal Mig phenotype. We chose to revert *daf-12(rh61)* first, because *daf-12* LBD mutant *(rh61)* are thought to act proximal to *din-1* within the presumed pathway. Second, in part 3 of this chapter we showed that DIN-1 physically interacts with *daf-12(rh61)* mutant protein in a two hybrid assay (Figure 16). Third, in part 4 of this chapter, we showed that *din-1RNAi*

suppresses the *daf-12(rh61)* gonadal mig phenotype. In addition, a screen for reversion the Mig phenotype is easy to score.

Genetic evidence suggests that together with *din-1*, *daf-12(rh61)* acts like a repressor to block the transcription of the target genes. As a result, gonadal outgrowth is delayed giving the Mig phenotype. When DIN-1 is absent, *daf-12(rh61)* no longer acts as a repressor and normal gonadal development is restored. Therefore, screening for revertants of the Mig phenotype should yield *din-1* mutants and other components of a corepressor complex. We also expect intragenic *daf-12* mutants that lose DNA binding activities since this should disrupt repression, too.

EMS mutagenesis of approximately 30000 genomes gave rise to nineteen non Mig lines. Thirteen of them were linked to the X-chromosome, Daf-d and probably *daf-12* intragenic alleles (Figure 20). Six of them were extragenic. These lines were tested for linkage to *dpy-10*, which maps 5.6 units away from *din-1* (Figure10). Four of the six alleles, *dh118, dh128, dh149* and *dh127,* showed linkage. Two of them were unlinked. We performed a second EMS mutagenesis where we screened for revertants of the *daf-12 (rh274)* Daf-c and Mig phenotype. Like *daf-12(rh61), daf(rh274)* affects the DAF-12 LBD. Mutagenesis of 30 000 genomes gave rise to one *din-1* mutation, *dh181.* Another *din-1* allele, *sa1262,* (provided by Jie Li, University of Washington, Seattle), which was isolated in a screen for suppressors of the Daf-cphenotypes of *npc-1; npc-2* double mutants (Niemann-Pick homologs 1 and 2). Sequence analyses confirmed that for all six alleles the affected gene was *din-1* (Table 12 and Figure 13B). *din-1(dh149)* has an 10 nucleotide deletion at position of bp 33150 according to the cosmid F07A11, causing a frame shift at position of aa. In *din-1(dh127)* a glutamine is transformed into a stop codon at position of aa 41 in the *din-1* isoform D. The *din-1* mutants *(dh118)* and *(dh128)* both have a stop codon at the same position, transforming an arginine into a stop codon at aa 303. Both mutants are independent, indicating that the region might be a hot spot for mutations. 16 that results in a stop codon 45 aa downstream. In *dh181,* a glycin is transformed into a stop codon at position of aa 77. Interestingly, sequence analyses revealed that *sa1262* harbours a point mutation in the predicted promotor region of the *din-1* isoform D at position of bp 34023 in F07A11 that is not comprised in the predicted open reading frame. The other five *din-1* alleles cluster in exon 18 (Table 12, Figure 12B). Remarkably, this region corresponds to the DAF-12 interaction domain that we identified in the yeast-two hybrid

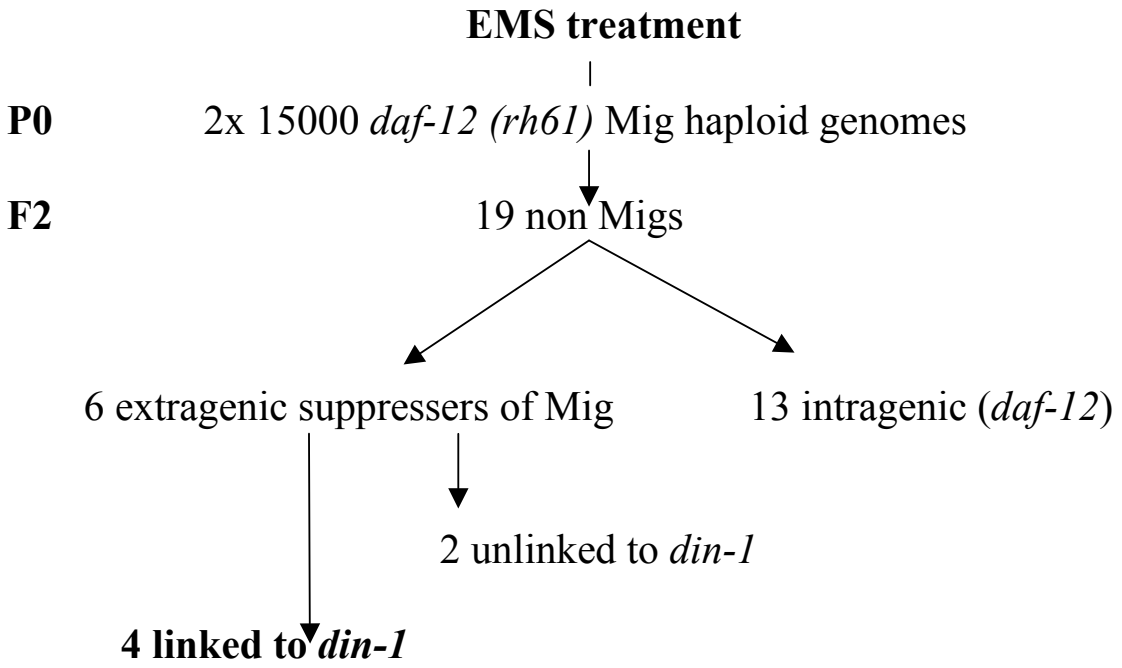

Figure 20) EMS mutagenesis screen for *daf-12 (rh61)* revertants

Table 12) *din-1* mutants

Allele	**Position according to DIN-1D**	Location according to F07A11	source
dh127	Q 41 stop	Exon 18 cag-tag at 33086	*daf-12(rh61)* revertant screen
dh118	R 303 stop	Exon 18 cga-tga at 32300	*daf-12(rh61)* revertant screen
dh128	R 303 stop	Exon 18 cga-tga at 32300	*daf-12(rh61)* revertant screen
dh149	frame shift at 16 stop codon at 61	Exon 18; 33150-33160 deletion	*daf-12(rh61)* revertant screen
dh181	Q 118 stop	Exon 18 gga-tga at 33206	*daf-12(rh274)* revertant screen
sa1262		putative promotorregion upstream of exon 18 at 34023	screen for *npc-1 npc-2* revertants; James Thomas, personnal communication

screens, suggesting that these alleles disrupt the DIN-1-DAF-12 association. Presumably, none of the isolated *din-1* alleles are a null, because isoforms A, B and C are intact.

Table 13) Interactions of *din-1* mutants with *daf-12(rh61);* isolated as *daf-12 rh61* revertants

	% L3 seam[1]	% Adult seam [2]	% reflexed dtc[3]	Dauer Formation	% avarage Brood Size
N2	100	100	100	Non-Daf	100
daf-12(rh61)	10	80	0	Daf-d	14
din-1(dh127)	100	100	100	Non-Daf	78
din-1(dh118)	n.d.	n.d.	n.d	n.d	104
daf-12(rh61); din-1(dh128)	82	100	100	Daf-d	63
daf-12(rh61); din-1(dh118)	54	99	100	Daf-d	49
daf-12(rh61); din-1(dh149)	50	99	100	Daf-d	n.d.
daf-12(rh61); din-1(dh127)	62	99	100	Daf-d	44
daf-12(rh61); din-1RNAi	87	98	100	Daf-d	n.d.

[1] n=10 animals (110 cells)
[2]n=25 animals
[3] n=25 animals

Table 14) Interactions of *din-1* mutants isolated as *daf-12(rh61)* revertants with Daf-c mutants

Genotype	% Daf-c[1]	Genotype	% Daf-c[1]
N2 (n=>500)	0		
din-1(dh127) (n=>500)	0		
daf-12(rh273) (n=500)	18	*daf-12(rh273); din-1(dh127) (n=1005)*	0
daf-9(dh6) (n=584)	100	*daf-9(dh6);din-1(dh127 (n=1129)*	0
daf-2 (m41) (n=741)	100	*din-1(dh127),daf-2(m41)(n=506)*	0.4
daf-2(e1368) (n=421)	100	*din-1(dh127):daf-2(e1368)(n=418)*	0
daf-2(e1370) (n=429)	96[2]	*din-1(dh127):daf-2(e1370) (n=88)*	99[2]
daf-7(m62) (n=920)	100	*daf-7(m62; din-1(dh181) (n=803)*	24

[1] Daf-c full dauers, partial dauers or L2ds
[2]Remaining fraction arrest as L1s

4.5.2 *din-1* phenotypes

Isolated *din-1* alleles resembled *din-1RNAi* (Table 13). First, on their own they had no observable phenotype. Second, they potently suppressed the Daf-c phenotype of dauer pathway mutants. Third, they suppressed the gonadal Mig and the alae gap phenotype of *daf-12(rh61)* mutant (Table 13, 14, Figure 21).

For further phenotypic analyses of the *din-1* alleles, we examined the percentage of L3 and adult seam cells, the reflection of the distal tip cell (dtc), their ability to form dauers and the brood size. We compared these data with those from N2, *daf-12(rh61)* and *din-1; daf-12(rh61)* double mutants (Table 13).

The percentage of L3 seam cells in *daf-12(rh61)* is 10% of wild type. *din-1(dh127*) L3 seam cell number is identic with wild type. In *daf-12(rh61)*; *din-1* double mutants, the number of L3 seam cells varies between 50% *(dh149)* and 82% *(dh128)* of wild type, indicating that *din-1* suppresses L3 seam cell formation in *daf-12 (rh61)* mutants. Remarkably, *daf-12(rh61*) forms

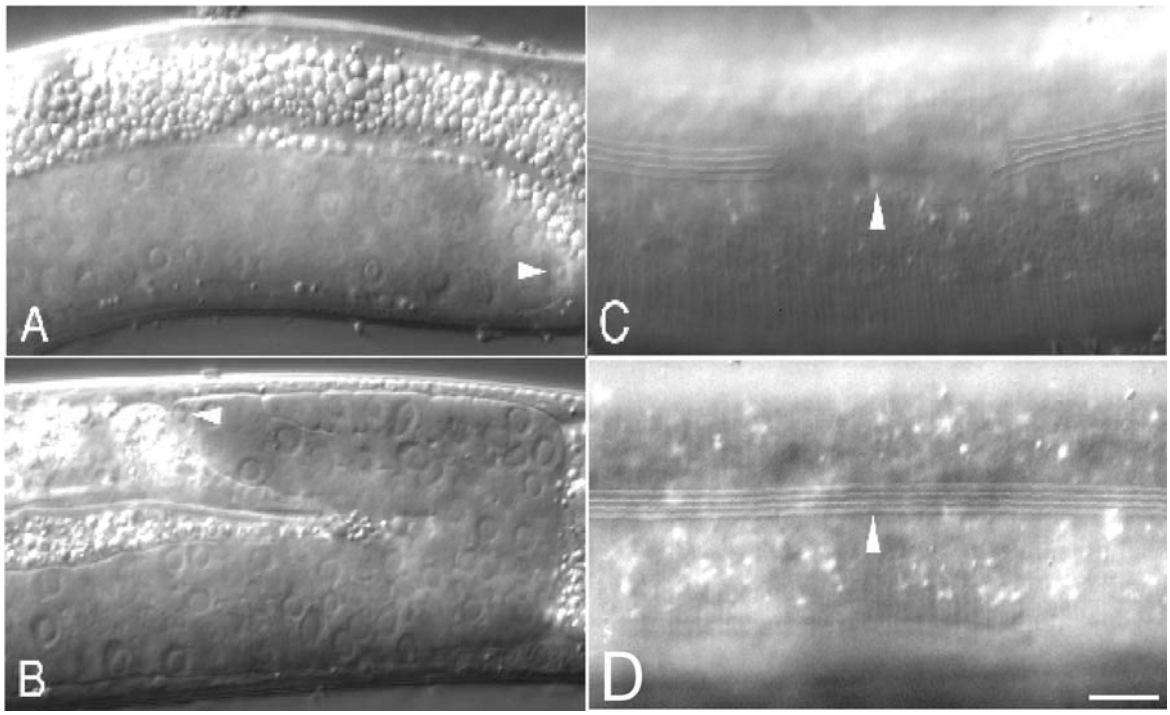

Figure 21) The *din-1* allele *dh127* suppresses the *daf-12(rh61)* Mig and alae gap phenotype in double mutants, left lateral aspect, scale bar is 10 µM **A)** *daf-12(rh61)*, larval stage 4 after 2 days of growth at 20°C. Unreflected gonad arm. **B)** Reflected gonad arm and distal tip cell in *daf-12(rh61) din-1(dh128)* double mutants. The distal tip cell of the gonad is marked with an arrowhead. **C)** Alae gap phenotype of young adult *daf-12(rh61)* mutant after 4 d of growth at 20°C. **D)** complete alae in *daf-12(rh61) din-1(dh128)* double mutants.

87% of wild type L3 seam cells on *din-1RNAi* plates, indicating that *din-1RNAi* suppresses the *daf-12(rh61)* L3 seam cell phenotype more efficiently than the tested *din-1* alleles. We also looked at the alae gap phenotype in the *din-1* mutants (% adult seam in Table 13). Thepercentage of adult seam cells in *daf-12(rh61)* is 80% of wild type. *din-1(dh127)* adult seamcell number is identic with wild type. The percentage of adult seam cells in *daf-12(rh61); din-1* double mutants varies between 98% and 100% of wt, indicating that *din-1* suppresses also the adult seam cell formation in *daf-12 (rh61)* mutants.

In wild type worms, 100% of gonads are reflected. By contrast, all *daf-12(rh61)* mutants do not show gonadal reflexion at all. *daf-12(rh61); din-1* double mutants as well as *daf-12(rh61)* mutants grown on *din-1RNAi* had reflected gonads (Table 13, Figure 21), strongly indicating that *din-1* inhibits appropriate gonadal development in *daf-12 (rh61)* mutants.

daf-12(rh61) has only 14% of wild type brood size. The average broodsize in *din-1* mutants was almost identical to wt (*dh118*, 105% of wt) or slightly decreased (*dh 127*, 78% of wt). The brood size of *daf-12(rh61)*/*din-1* double mutants varied between 44% and 66.1% compared

with wild type, indicating that in *daf-12 (rh61)* mutants, *din-1* diminishes the regular brood size.

In summary, all the tested *daf-12(rh61)* phenotypes are partly suppressed by *din-1*. Allele *(dh128)* has the strongest effects. This mutant has the same change as *dh118* but differs in phenotype. It was possible that it had a second mutation. However, when we sequenced the *din-1(dh128)* coding region, we could not find another match.

To test the influence of *din-1* mutants on dauer formation, we also scored interactions of *din-1*(*dh127)* with the Daf-c mutants *daf-12(rh273), daf-2(m41), daf-9(dh6), daf-2(e1368), daf-2(e1370)* and *daf-7(m62)* (Table14). At 25°C, N2 and *din-1(dh127)* do not form dauers. *daf-9(dh6), daf-12(m41), daf-2(e1368)* formed 100% dauers. This phenotype was nearly 100% suppressed in each double mutant with *din-1*(*dh127)*. *daf-12 (rh273)* forms 18% dauers, whereas *rh273; din-1(dh127)* never formed dauers. Consistent with our RNAi results, *daf-2(e1370)* formed 96% dauers, and the double mutant with *din-1(dh127*) formed 99% dauers. *daf-7(m62)* forms 100% dauers, in *din-1(dh181); daf-7(m62)* we scored 24% dauers, indicating that *din-1* might only partly suppresses *daf-7* Daf-c phenotypes. In contrast, *din-1RNAi* suppressed *daf-7(e1372)* Daf-c phenotypes almost completely (Figure 17).

To test whether the postulated *din-1* isoform D is sufficient for the rescue of the *din1(dh127); daf-2(e1368)* non-Daf phenotype, we microinjected the plasmid Topo-Din-1D, containing the genomic *din-1D* region and a putative 3.4kb promotor region. 39.5% of the F2 generation restored the Daf-c phenotype, seen in *daf-2(e1368)* mutants (n=343).

However, restoration of the Daf-c phenotype was partial. Pharynx and alae showed dauer character, whereas the gonad was not suppressed. In some cases gonadoblasts divided and the distal tip cell migrated. We conclude, that *din-1* isoform D is partly sufficient to rescue *din-1(dh127)*. Conceivably, a longer promotor region gives a more complete rescue.

It is possible that *din-1* acts by destabilizing DAF-12, thus causing suppression of Daf-c and heterochronic phenotypes. To examine this possibility we looked at *daf-12::*GFP in a *din-1(dh127)* background. We saw no obvious change in expression (n=20). We conclude that din-1 suppresses Daf-c mutants by another mechanism.

To test if the enhancement of the *dre-1* gonadal Mig phenotypes observed in RNAi experiments is reproducible, we made *dre-1(dh99); din-1(dh127)* double mutants. In all 50 scored animals, we did not see a Mig phenotype. Conceivably, RNAi knock down results in a more severe phenotype.

4.6 Aging experiments with DIN-1

Mutations in the *C. elegans* Insulin/IGF receptor DAF-2 leads to an extension of life span. *daf-2* class I alleles e.g. *daf-2(e1368)* live around 2-fold longer than wild type; *daf-2* class II mutants *like daf-2(e1370)* live up to 3-fold longer than wild type animals. Moreover, *daf-12;daf-2* (class II) double mutants live four times longer than wild type animals (Kenyon et al., 1993; Gems et al., 1998). We asked whether *din-1* could influence the longevity phenotypes of *daf-2*. We found that *din-1(dh118)* alone lived as long as wild type. Double mutants with daf-2*(e1368)* lived slightly shorter than daf-2*(e1368)* alone, whereas *din-1(dh118)* had no effect on *daf-2(e1370)* (Figure 22).

In preliminary aging experiments with *din-1*RNAi, we observed a shortened life span of *din-1(dh127);daf-2(e1368)* (data not shown). To confirm this, we set up an aging screen with *din-1(dh127),* and *din-1(dh127);daf-2(e1368)*, and *din-1(dh127);daf-2(e1370)* double mutants. All strains were grown on *E. coli* HT115 bacterial lawn, expressing *din-1 RNAi* or carrying the empty vector only. We saw no effect on life span with *din-1*(*dh127)* alone. We also observed no effect with *din-1 (dh127);daf-2e1368)* double mutants (Figure 23). By contrast, we found

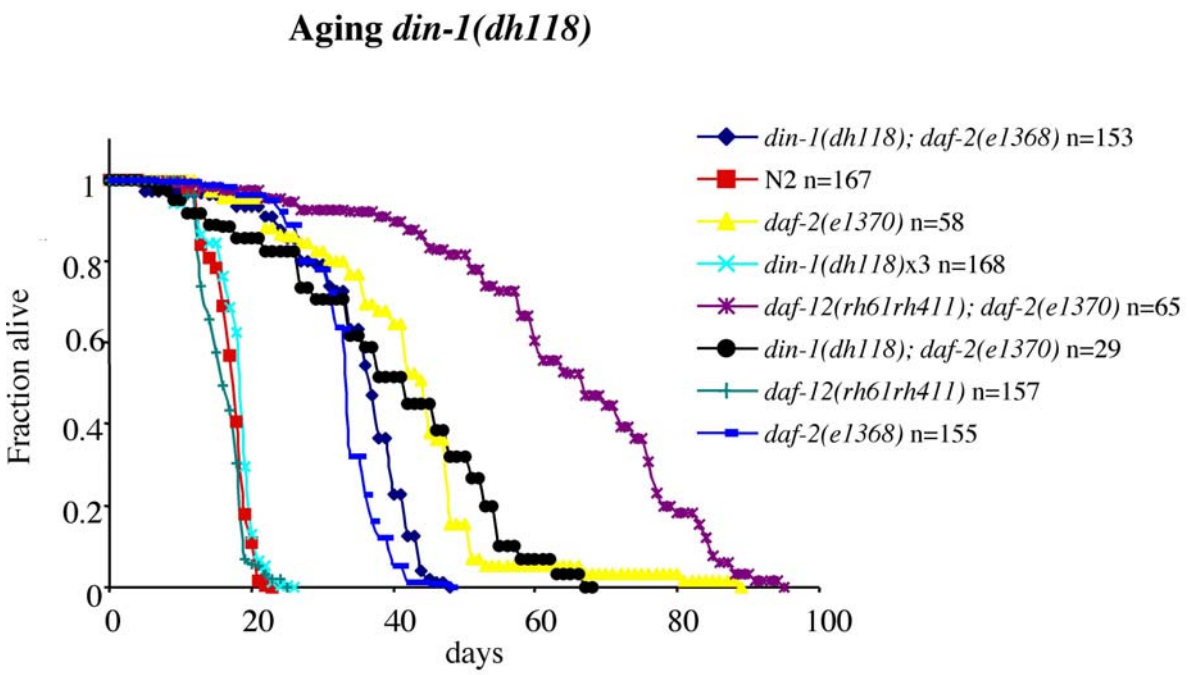

Figure 22) Aging experiments with the *din-1* allele *dh118*, N2, *daf-2(e1370),* and the double mutants *daf-12(rh61rh411);daf-2(e1370), daf-2(e1368);din-1(dh118), daf-2(e1370);din-1(dh118).*

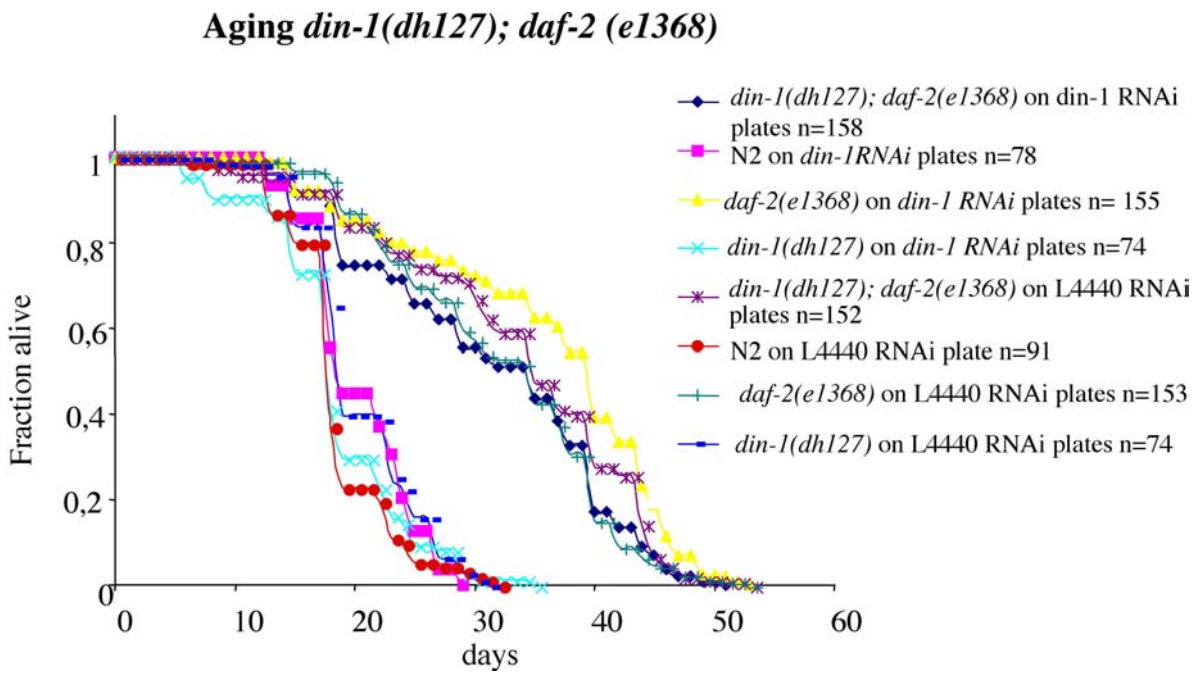

Figure 23) Aging experiments with the *din-1* allele *dh127*, N2, *daf-2(e1368), daf-2(e1370),* and the double mutant *daf-2(e1368);din-1(dh127).* Worms were grown on HT115 lawn, transformed with L4440 or on HT 115 lawn expressing *din1RNAi*

.

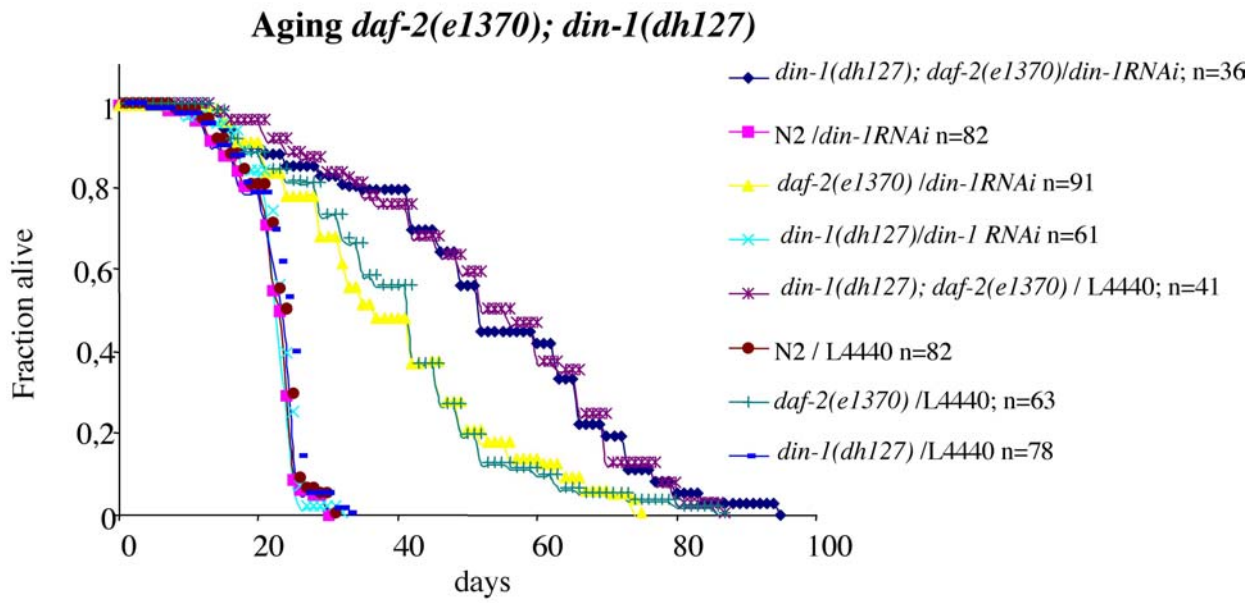

Figure 24) Aging experiments with the *din-1* allele *dh127*, N2, *daf-2(e1370),* and *daf-2(e1370)/din-1(dh127).* Worms were grown on HT 115 lawn, transformed with L4440 or on HT 115 lawn expressing *din-1RNAi*.

Table 15) Aging experiments with the *din-1* allele *dh127*, N2, *daf-2(e1370),* and *daf-2(e1370)/din-1(dh127)* on *L4440* and *din-1RNAi* plates.

Aging *din-1(dh127)daf-2(e1370)/din-1RNAi*						
	mean	median	max	stdev	#	p student11 T test
din-1(dh127); daf-2(e1370)/ din-1RNAi; n=36	50,4	50,5	95	21,9	36	8E-04; *din-1(dh127*); *daf-2 (e1370)/din-1RNAi* versus *daf2(e1370) /din-1RNAi*
N2 / *din-1RNAi* n=82	22,1	23,5	30	4,5	82	
daf-2(e1370)/din-1RNAi n=91	37,0	34	75	16,1	91	
din-1(3dh127)/ din-1 RNAi n=61	23,1	24	32	3,8	61	
din-1(dh127);daf-2(e1370)/L4440 n=41	47,8	47	87	22,6	41	0,003; *din-1(dh127); daf-2(e1370)* / L4440 versus *daf-2(e1370)*/ L4440
N2 / L4440 n=82	23,1	24,5	31	4,5	82	
daf-2(e1370) /L4440 ;n=63	35,8	33	87	17,1	63	
din-1(dh127) /L4440 n=78	23,3	25	33	5,1	77	

that *din-1(dh127)* increased the mean life span of *daf-2(e1370)* by 35.1%, the maximal life span was equal. We observed a similar effect on *din-1RNAi* plates. *din-1(dh127)* increased the mean life span of *daf-2(e1370)* by 36.6%. The maximal life span of *daf-2(e1370)* was 75 days, and din*(dh127);daf-2(e1370)* 95 days. We assume that for a critical point of time in the experiment, the induction of the din-1 RNAi did not work. We are now confirming those results on OP50 plates (Figure 24, Table 5).

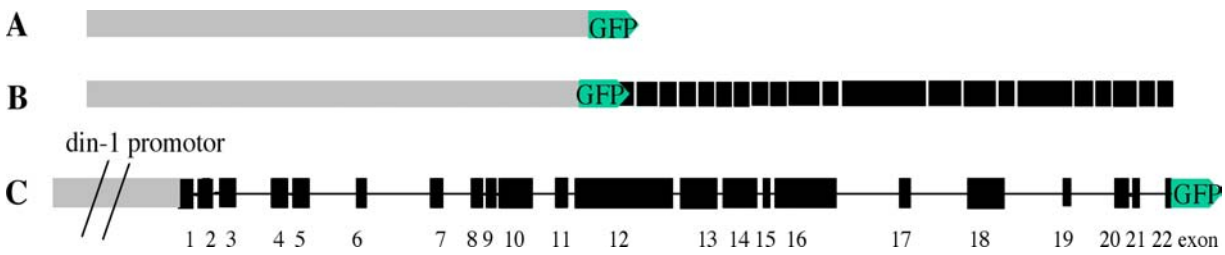

Figure 25) *din-::*gfp fusion constructs. A) L3781::*din-1* promotor, the *din-1* promotor region is fused to gfp in L3781. **B)** cDNA from *din-1* isoform A and *din-1* promotorregion is fused to gfp in L3781. **C)** Genomic *din-1* C-terminal fused to gfp via homolog recombination in yeast.

4.7 DIN-1 expression

To investigate DIN-1 expression, we made three different DIN-1::gfp constructs (Figure 25). To score DIN-1 promotor activity, we fused the region 8 kB upstream of the *din-1* 5'end to gfp (Figure 25A). We detained 3 extragenic gfp(+) F2 lines, which gave similar expression patterns. DIN-1 is expressed throughout all developmental stages from embryo to adult hermaphrodites, males as well as dauer larvae (Figure 26). DIN-1 expression is seen in the nervous system (Figure 26A, F, G, H), pharynx (26F, G), intestine (Figure 26B), distal tip cell of the gonad (26C), L3 seam cells (26D) and in the adult vulva (26E). Moreover, we also observed expression in muscle and hypodermis (not shown). Interestingly, all the tissues with DIN-1 expression are remodelled during dauer formation. In particular, *din-1* is expressed in cells phenotypically affected by *daf- 12* mutants such as the distal tip cells and the seam cells (Figure 26C, D).

To determine *din-1* subcellular localisation, we cloned a 7.7 kB cDNA fragment containing *din-1* isoform A into the gfp promotor vector (Figure 25B) and microinjected it into worms. We obtained four GFP(+ F2 lines. We confirmed that the construct is expressed within the nucleus of different cell types. In particular, it is expressed in seam, hypodermis, vulval cells, ventral cord and peripheral neurons (Figure 27A, B), body muscles, pharynx (Figure 27A, B), intestine and somatic gonad.

We also tagged the genomic 3'end of DIN-1 with GFP by using homologous recombination of a short 3'end genomic fragment that was cloned into a GFP vector in a yeast strain carrying a YAC that encodes DIN-1 (Figure 25C). We could not detect gfp signals in the transgenic animals.

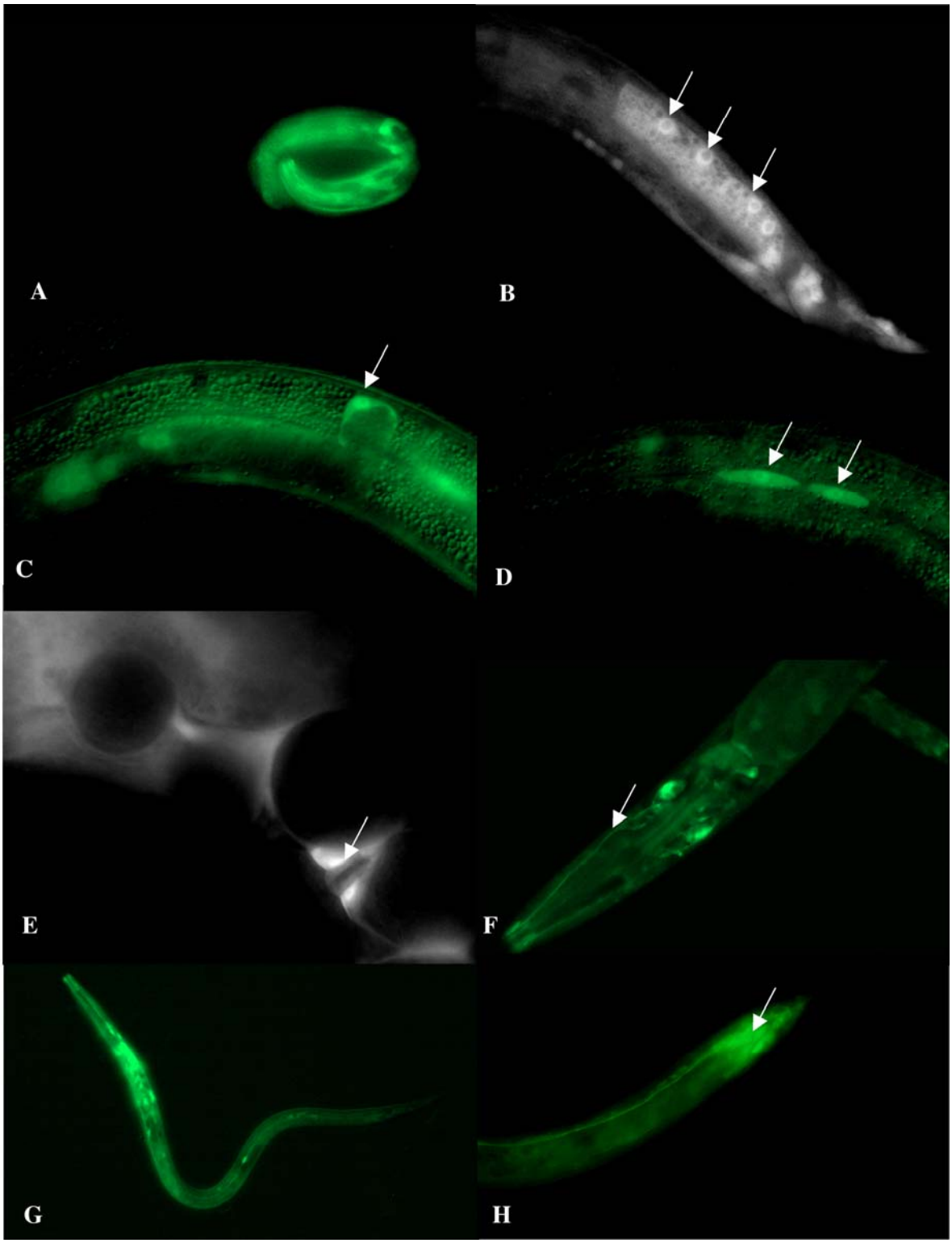

Figure 26) Expression of a Din-1::gfp promotor construct at different developmental stages. A) Embryo (100x), **B)** L3, intestinal cells; nuclei are marked with arrows (63x). **C)** L3 distal tip cell of the gonad (arrow) (63x), **D)** L3 seam cells (arrow) (63x), **E)** adult vulva (100x), **F)** Neurons in the head region of an old adult (arrow) (40x), **G)** dauer larvae (40x), **H)** adult male tail (40x).

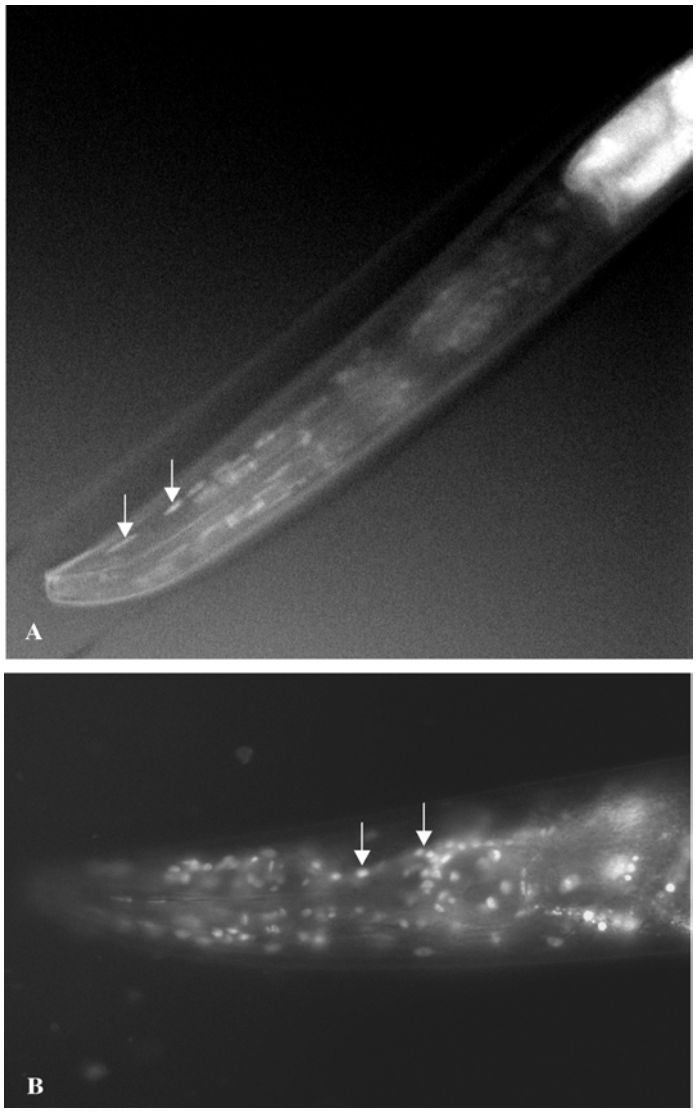

Figure 27) DIN-1 is expressed in the nucleus; gfp expression of a DIN-1AcDNA::gfp fusion protein. A) dauer larvae, head region, arrows indicate nuclei of pharyngal cells (100x). **B)** Adult, head region (63x), arrows indicate nuclei of pharyngal cells.